

AD-A151 840

THE EFFECTS OF ATMOSPHERIC TURBULENCE ON AN AIR-TO-AIR
OPTICAL COMMUNICATION LINK(U) AIR FORCE INST OF TECH
WRIGHT-PATTERSON AFB OH SCHOOL OF ENGI.. J N KANAVOS

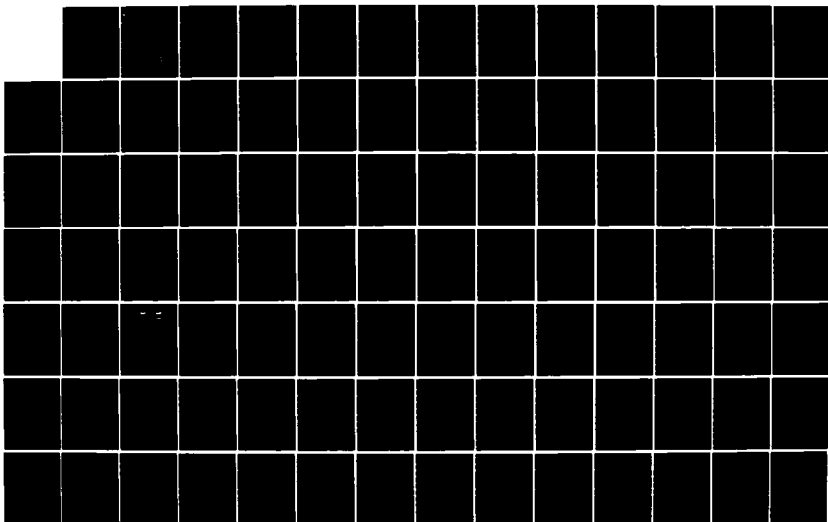
1/8

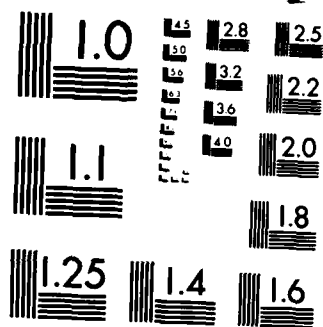
UNCLASSIFIED

DEC 84 AFIT/GE/ENG/84D-38

F/G 17/2

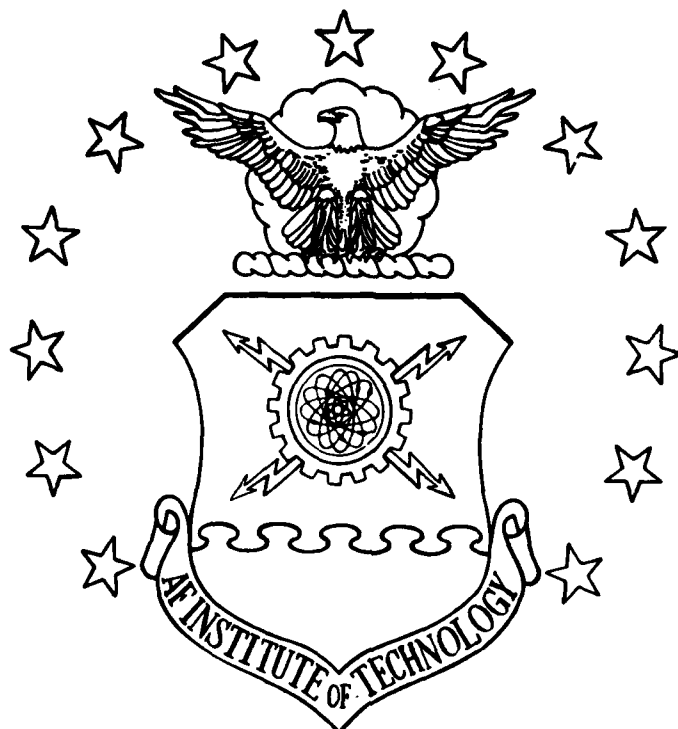
NL





MICROCOPY RESOLUTION TEST CHART
NATIONAL BUREAU OF STANDARDS-1963-A

AD-A151 840



DTIC

①

THE EFFECTS OF ATMOSPHERIC TURBULENCE
ON AN AIR-TO-AIR OPTICAL
COMMUNICATION LINK

THESIS

JAY N. KANAVOS
CAPTAIN USAF

AFIT/GE/ENG/84D-38

DISTRIBUTION STATEMENT A

Approved for public release;
Distribution Unlimited

DEPARTMENT OF THE AIR FORCE
AIR UNIVERSITY

AIR FORCE INSTITUTE OF TECHNOLOGY

Wright-Patterson Air Force Base, Ohio

DTIC
ELECTE
MAR 29 1985

S B

85

03

13

174

REPRODUCED AT GOVERNMENT EXPENSE

DTIC FILE COPY

AFIT/GE/ENG/84D-38

THE EFFECTS OF ATMOSPHERIC TURBULENCE
ON AN AIR-TO-AIR OPTICAL
COMMUNICATION LINK

THESIS

JAY N. KANAVOS
CAPTAIN USAF

AFIT/GE/ENG/84D-38

DTIC
ELECTE
MAR 29 1985
S B

DISTRIBUTION STATEMENT A

Approved for public release;
Distribution Unlimited

AFIT/GE/ENG/84D-38

THE EFFECTS OF ATMOSPHERIC TURBULENCE ON AN
AIR-TO-AIR OPTICAL COMMUNICATION LINK

THESIS

Presented to the Faculty of the School of Engineering
of the Air Force Institute of Technology

Air University

In Partial Fulfillment of the
Requirements for the Degree of
Master of Science in Electrical Engineering

Jay N. Kanavos, B.S.

Captain USAF

December 1984

Approved for public release; distribution unlimited

Preface

The purpose of this thesis was to evaluate the performance of an air-to-air optical communication link in the presence of atmospheric turbulence. By varying certain performance parameters (i.e. aircraft speed and altitude), a variety of communication links can be evaluated. Knowing how a certain link will perform can aid in the determination of the maximum reliable communication range between aircraft. I feel that the results obtained from this project will provide some insight into the limitations of optical communications between aircraft.

While writing this thesis, I find myself looking back over the months and realizing that the contributions made by others, whether great or small, were an enormous help to me. Recognizing this, I would like to express my gratitude to my advisor, Dr. Vaqar Syed, for his dedicated technical direction throughout the entire project. In addition, I would like to thank Majors Kenneth G. Castor and Richard J. Cook for their greatly appreciated advise and counseling. Special thanks is due to First Lieutenant Linden Mercer, AFWAL/AAAI-1, Wright-Patterson AFB, Ohio, for providing both this thesis topic and an education on the subject of turbulence and optical equipment limitations.

Finally, I wish to express my sincerest appreciation and gratitude in the dedication of this thesis to my wife,

Michelle. Her support, love, and patience during the period of this effort has made this thesis a special success.

Jay Nicholas Kanavos



Accession For	
NTIS	<input checked="checked" type="checkbox"/>
DTIC	<input type="checkbox"/>
Unan	<input type="checkbox"/>
Just	<input type="checkbox"/>
By	
Initial	
Availability Code	
Dist	Special
A-1	

Table of Contents

	Page
Preface	ii
List of Figures	vii
List of Tables	x
Abstract	xi
I Introduction	1
Background	1
Problem Statement	3
Approach	4
Limitations	4
Organization	5
II Elements of an Optical Communication System	7
Optical Communication System Model	7
Physical Components	9
The Optical Transmitter	9
The Optical Receiver	10
The Optical Channel	13
The Refractive Index Structure Constant	15
Probability Distribution of Intensity Fluctuations	18
Derivation of the Mean and the Variance	21
Power Spectral Density	27
Development of the Denormalized Power Spectral Density	29
Summary	30
III Mathematical Derivation of the Simulation	31
Introduction	31
Simulation of the Input Signal	32
Simulation of the Atmospheric Channel	33
Background Radiation	44
Optical Beam Divergence	46
Simulation of the Receiver	48

Determination of the Threshold Level	51
Summary	55
.IV Results of the Simulation	56
Introduction	56
Performance of the Baseline System	58
Performance of the Actual Optical Link	63
Summary	79
V Conclusions and Recommendations	80
Conclusions	80
Recommendations	82
Appendix A:	84
Data Points for Link Altitude of 10,000 ft	84
Data Points for Link Altitude of 20,000 ft	85
Data Points for Link Altitude of 30,000 ft	86
Appendix B: Fortran Computer Listing	87
Bibliography	94
Vita	95

List of Figures

Figure		Page
1	Block Diagram of an Optical Communication System	8
2	Receiver Configuration	11
3	Experimental C_n^2	16
4	C_n^2 vs. Altitude	18
5	Communication System Block Diagram	20
6	Maximum Propagation Path Length of Optical Beam Not in Saturation	20
7	Lognormal Distribution for a Variety of σ_X^2 Values	25
8	Phenomenon of Decreasing Variance in the Saturation Region	26
9	Normalized Power Spectral Density of the Intensity Fluctuations	28
10	Denormalized Power Spectral Density	30
11	Communication System Model	31
12	Black Box Analogy	34
13	Block Diagram of the Gujar Kavanaugh Technique	35
14	FFT of the Sequences $Z(n)$ and $Y(n)$	45
15	Divergence of the Optical Beam as the Path Length Increases	47
16	Theoretical Bit Error Rate for an Altitude of 10,000 Ft	59
17	Theoretical Bit Error Rate for an Altitude of 20,000 Ft	60
18	Theoretical Bit Error Rate for an Altitude of 30,000 Ft	61

19	Turbulence Affected Optical Link Altitude: 10,000 ft Aircraft Speed: 425 knts Data Rate: 20,000 bps	64
20	Turbulence Affected Optical Link Altitude: 10,000 ft Aircraft Speed: 475 knts Data Rate: 20,000 bps	65
21	Turbulence Affected Optical Link Altitude: 10,000 ft Aircraft Speed: 425 knts Data Rate: 40,000 bps	66
22	Turbulence Affected Optical Link Altitude: 20,000 ft Aircraft Speed: 425 knts Data Rate: 20,000 bps	67
23	Turbulence Affected Optical Link Altitude: 20,000 ft Aircraft Speed: 475 knts Data Rate: 20,000 bps	68
24	Turbulence Affected Optical Link Altitude: 20,000 ft Aircraft Speed: 425 knts Data Rate: 40,000 bps	69
25	Turbulence Affected Optical Link Altitude: 30,000 ft Aircraft Speed: 425 knts Data Rate: 20,000 bps	70
26	Turbulence Affected Optical Link Altitude: 30,000 ft Aircraft Speed: 475 knts Data Rate: 20,000 bps	71
27	Turbulence Affected Optical Link Altitude: 30,000 ft Aircraft Speed: 425 knts Data Rate: 40,000 bps	72
28	Representation of Possible Turbulence Factor Sequences	75

29

Representation of the Turbulence
Factor Sequences for an Altitude
of 20,000 ft and a 70 km Path
Length

76

List of Tables

Table		Page
I	Advantages and Disadvantages of an Unguided Optical Communication System	8
II	Chebychev Filter Orders for a Variety of Optical Propagation Environments	38
III	Parameters of the Communication Links Used	57
IV	Transmitter and Receiver Characteristics	57
V	Maximum Ranges for the Baseline Link and the Turbulence Affected Link	73

Abstract

This report presents an analysis of the performance of an air-to-air optical communication link in the presence of atmospheric turbulence. As aircraft travel through the atmosphere, they encounter regions of atmospheric turbulence. While harmless to radio frequency (RF) communications, these regions of turbulence can cause both intensity and phase fluctuations within an optical beam. As a result, the communication link bit error rate rises.

To evaluate the performance of such a link, a computer simulation was developed. By varying such parameters as the speed of the aircraft, its altitude, and propagation path length, a determination could be made about link performance.

The results obtained from the simulation showed that atmospheric turbulence plays a significant role in determining link performance. It was found that the maximum reliable communication ranges, of those links affected by turbulence (real life situation) were degraded approximately 50 - 60 percent over those links not affected. It was also determined that reasonable changes in aircraft speeds had no significant impact on the bit error rates, while an increase in altitude greatly increased the maximum reliable communication ranges.

The Effects of Atmospheric Turbulence on an Air to Air Optical Communication Link

1. Introduction

Background

The attention given to optical communication systems over the past decade has been staggering. There has been a tremendous effort under way to develop workable system designs for potential communication links. To do this, researchers have found that understanding the detrimental effects that the atmosphere has on optical wave propagation is essential in determining the "condition" of the received wave. To date, researchers have attempted to describe the effects which influence an optical beam in both terrestrial and earth-to-space satellite links. However, little work has been done in evaluating the effects which influence an air-to-air optical communication link.

As an aircraft travels through the atmosphere, it encounters regions of turbulence. Turbulence can be described as the violent mixing of one substance with another substance. In this case, these substances are the ambient layers of the earth's atmosphere. Throughout the entire atmosphere, the prevailing winds constantly mix warmer air with cooler air. The result is a potpourri of thermal air pockets, or eddies, flowing within the

atmosphere. The temperature variations between these eddies are very small (on the order of .1-1 degree C); however, they are large enough to cause index of refraction fluctuations. Since each eddy consists of a different temperature, its index of refraction will vary. Thus, each eddy's index of refraction will consist of a slightly different value than that of its neighbor. Although these differences are typically small (on the order of 10^{-6}), they can have a significant impact on the optical beam.

As an optical beam passes from one eddy to another, the changes in the indices of refraction cause the beam to bend. Since this beam passes through many eddies, parts of the beam may travel through more eddies than other parts of the beam. As a result, the optical beam will arrive at the detector with both intensity and phase fluctuations.

These fluctuations, known as scintillations, vary randomly with time. Thus, the turbulence-induced intensity scintillations become stochastic processes. Since these scintillations are not deterministic, they must be analyzed using statistical mathematics. Therefore, in order to determine the "condition" of the received optical beam, the statistics of these scintillations must first be determined.

In determining these statistics, there are three quantities which must be specified: the probability distribution, its mean, and its variance. It is generally agreed that the probability distribution of the intensity

fluctuations assumes a lognormal distribution. However, this assumption can only be valid when the optical beam is not operating within the so called "saturation region." If the beam is operating within this region, then its intensity fluctuations will no longer exhibit lognormal statistics. In fact, researchers have yet to determine what statistics are valid.

The lognormal distribution has two parameters: its mean and variance. It turns out that the mean is actually equal to the negative of its variance. Thus, this particular distribution is really a function of only one variable; its variance. The variance, however, is dependent on a variety of factors indigenous to the environment surrounding the transmitted optical beam. Such factors include: the propagation path distance, altitude, and time of day. Once this variance is computed, the statistics of the scintillations can be completely described.

Problem Statement

Atmospheric turbulence induces both intensity and phase fluctuations in the optical beam. These fluctuations will play a major role in degrading communication link performance, i.e. probability of bit error in digital communication systems will increase. As a result, mission essential optical communication links could be rendered inoperative under certain conditions. To determine the

reliability, and feasibility, of an air-to-air optical communication link, it will be necessary to determine those conditions, and/or system parameters, which will support reliable communications.

Approach

This thesis will be directed towards a simulation of the atmospheric effects which would influence an air-to-air optical communication link. In determining how this communication link will be affected, the bit error rates will be determined at various altitudes, propagation path lengths, and aircraft speeds. To do this, a computer model which simulates the transmission and detection of a binary signal through the turbulent optical channel, will be developed.

Limitations

The primary thrust of this thesis will focus on the effects of scintillation due to clear air turbulence. The following conditions will be assumed throughout this document:

1. Due to frequency stability factors inherent in local oscillators aboard aircraft, a direct detection scheme will be used. As a result, intensity fluctuations (rather than phase fluctuations) of the optical beam will be of primary concern.

2. The transmitted optical signal will consist of a sequence of 1's and 0's randomly transmitted through the atmospheric channel. This will simulate a binary information signal.

3. The optical beam will exhibit plane wave characteristics. This assumption limits the accuracy of the final results, but greatly reduces the mathematical complexity of the problem.

4. The optical beam between the two aircraft will be perpendicular to both aircraft. Also, both aircraft will be assumed to be at equivalent altitudes.

Organization

This thesis will be organized into five chapters and two appendices.

Chapter II will include a brief tutorial on optical communication systems. The characteristics of the turbulent channel will be discussed, as well as a mathematical derivation of its statistics.

Chapter III will describe the approach taken in producing the computer model, as well as the mathematical theory which justifies each of the various steps.

Chapter IV will present the results obtained from the simulation. These results will be based on a random sequence of 1's and 0's transmitted through the optical channel. An assessment of how the system probability of error is affected by atmospheric turbulence at various

altitudes, propagation path lengths, and aircraft speeds will also be included.

Chapter V will consist of both conclusions and recommendations that the author feels could improve the simulation.

The appendices will consist of the data points used to generate the performance curves, and the Fortran computer model program listing.

11. Elements of an Optical Communication System

Optical Communication System Model

The use of optical communication techniques has long been recognized as an effective means of communicating. Optical communication techniques have advanced from the use of beacon fires to shipboard blinker systems to the laser communication systems of today. Present laser communication systems have developed to such a point that they are not only practical for many applications, but offer some significant advantages over common radio frequency (RF) communications. However, optical communication links are not always the best choice for a given type of environment. The advantages and disadvantages of unguided optical communication systems are given in Table I.

The block diagram of a generalized optical communication system model is shown in Figure 1. In this model, the information signal can be thought of as a sequence of discrete symbols acquired from either a sampled waveform or a digital source. This discrete input signal is then modulated onto an optical carrier. The carrier is then transmitted as an optical light field, or beam, through the turbulent optical channel. At the receiver, the field is optically collected and processed, along with any interference and noise. Thus, the output signal is a corrupted version of the input signal.

Table I

Advantages and disadvantages of an unguided optical communication system (1:34)

Advantages	Disadvantages
High data rate capability	Uncertain reliability due to atmospheric conditions
Provides a good level of security	Requires very accurate pointing and tracking
Low power requirements	Less suited to broadcasting because of narrow beam
Relatively immune to crosstalk	Slightly higher level of noise in the received signal due to quantum nature of detection
Small antenna size	Possible eye hazard
No communication license required	
Exploits unused part of electromagnetic spectrum	

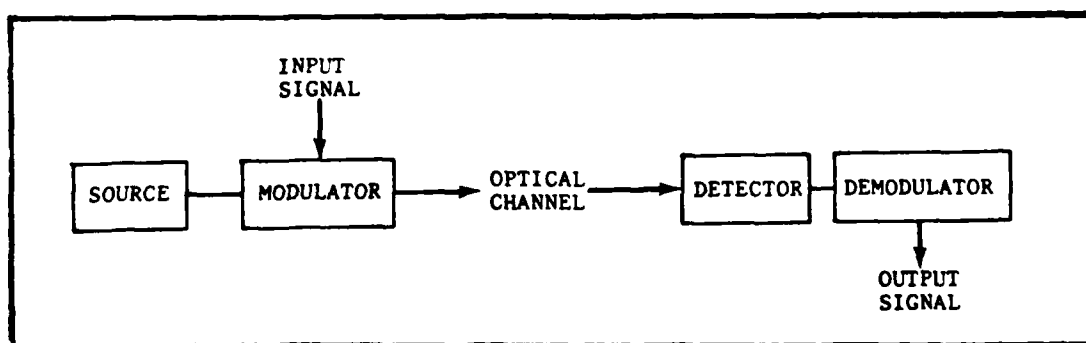


Figure 1. Block diagram of an optical communication system.

Since this thesis is concerned with the effects of atmospheric turbulence, the bulk of the discussion in this chapter will concentrate on the optical channel. However, to understand the entire optical communication system model, a basic understanding of its physical components is needed.

Physical Components

The main equipment components in the optical communication system are the transmitter and the receiver.

The Optical Transmitter

The optical transmitter can be represented as a cascade connection of an optical source, modulator, and antenna (lens system).

Optical sources (such as lasers and light emitting diodes (LED's)) produce the optical electromagnetic fields which act as the carrier for the information signal. Among some of the most popular laser sources used today are: Nd:YAG (1.06 μm), Nd:YAG (.53 μm), and CO₂ (10.6 μm and 9.6 μm).

In order to efficiently transmit information from one location to another, the information signal must first be conditioned in some manner. This conditioning is most commonly referred to as modulation. Modulation can be described as the process of combining an information signal, with a carrier, to construct a more suitable signal form for

transmission. There are a variety of optical modulation techniques available today. Among some of the schemes used are: intensity modulation (IM), phase modulation (PM), and polarization modulation (PL). In choosing which modulation scheme is best for a given type of system, there are several factors which must first be considered. For example, the kind of data to be transmitted and the type of detection equipment to be used are important considerations. If a direct detection receiver scheme were to be used, then some type of intensity modulation would be a logical choice. Once the system "environment" has been defined, then the choice of a modulation scheme can be made.

The Optical Receiver

The purpose of the receiver is to collect the incoming field of the optical beam. This is done by using a series of lenses which focuses the incoming field onto a photodetecting surface.

As can be seen in Figure 2, the receiving lens is located in the aperture plane, which has an area " A_r " and a focal length " f ." The lens focuses the received optical field onto the focal plane behind the lens. The focused field appears as a diffracted pattern in the focal plane. The photodetector is located in the focal plane, and responds to the portion of the diffracted field on its surface. The photodetector converts the field intensity of

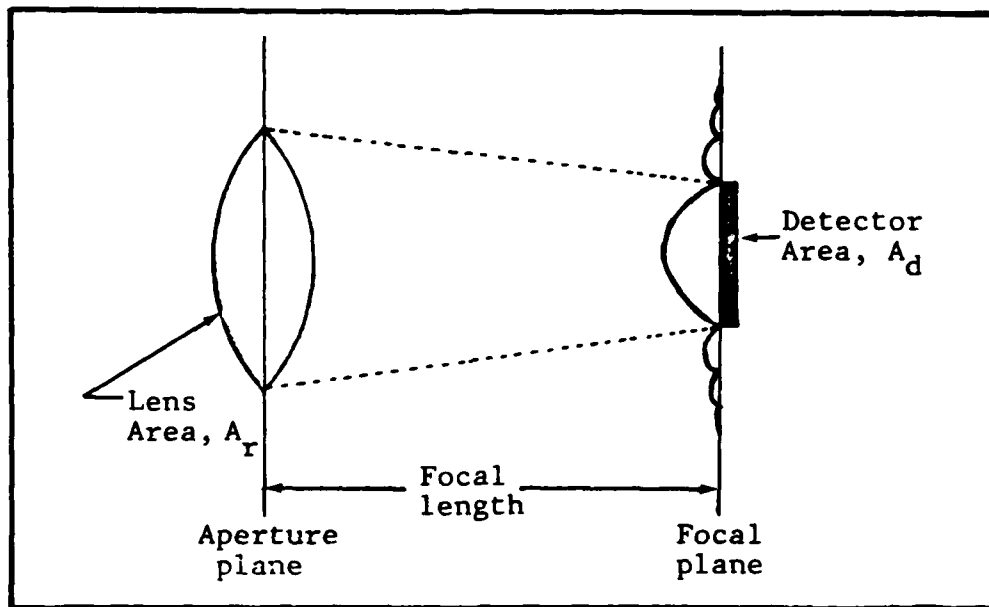


Figure 2. Receiver configuration (2:27).

the optical carrier into an electrical signal (2:27).

Typically, photodetectors fall into two classes: thermal and photon detectors. Since thermal detectors inherently have low bandwidth capabilities, they will be of little interest to us. Photon detectors, however, offer significant advantages over thermal detectors, and can be subdivided into classes according to their method of optical-to-electrical conversion. The most common conversions are: photoemission effect, photoconductive effect, photovoltaic effect, and the photoelectromagnetic effect.

The photoemissive effect involves the emissions of electrons from a vacuum tube cathode in response to optical excitation, while the latter three types of photo-effects

are all associated with semiconductor detectors. Here, the absorption of photons on the detector surface leads to a change in the concentration of charge carriers in the material. This change in the concentration of charge carriers produces the signal current.

After the photodetector has converted the optical beam into an electrical current, this current is then processed by some type of signal processor. Unfortunately, this processed signal is not the same signal that was transmitted. Disregarding the fact that the signal possesses turbulence-induced intensity fluctuations, it has also been corrupted by both thermal and shot noise, as well as dark current.

Dark current, thermal, and shot noises are all corruptive signals which originate within the receiver components. Each is random by nature and has its own set of statistics. All three forms of these noises are present in the photodetector, however, there are techniques which can be used to lessen their effects on a signal. For example, since the dark current's power spectra consists of an impulse located at $f=0$, it can be easily removed by a DC block filter.

Unfortunately, the effects due to thermal and shot noise cannot be eliminated as easily. The best that can be done is to limit the effects of one or the other: i.e. allow one to dominate over the other. Doing this allows the

potential system designer to use the statistical quantities of the dominating noise in determining the system probability of error and signal to noise ratios. This greatly simplifies the calculations, yet still provides a reasonable amount of accuracy in the determination of these quantities.

The Optical Channel

Temperature instability, within the earth's atmosphere, (resulting from rising warmer air mixing with descending cooler air) produces a state of turbulence. This turbulence causes fluctuations in the index of refraction within various neighboring eddies. Equation (1) (3:10) is the standard relation used to determine the value of the index of refraction at a particular point in both time and space.

$$n = 77.6(1+(7.52 \times 10^{-3})(\lambda^{-2}))(P/T)(10^{-6})+1 \quad (1)$$

where

n = index of refraction
 λ = wavelength of light
P = pressure (millibars)
T = temperature ($^{\circ}$ K)

By observing Eq. (1), it can be seen that as either the pressure or the temperature changes, so too does the index of refraction. As a result, eddies of varying indices of refraction are formed. Even though the sizes of these eddies can vary, researchers have found it convenient to classify them into two groups. These groups are known as outer and inner scale variations.

The outer scale variations, denoted L_o , is the name used to represent those groups of eddies which are physically larger in size. Values of L_o depend mainly on the height of these eddies above the ground. Typical values for L_o are 100 meters or $1/5$ the height above the ground - whichever is less (4:1527).

If there is a great deal of turbulence present in the atmosphere, then some of the outer scale variations can become unstable and begin to break apart. As a result, they become smaller. The resulting smaller eddies are called inner scale variations. Inner scale variations are usually only a few millimeters in size and denoted as l_o (4:1526-1527). To get a feel for the size of these inner scale variations, their dimensions can be approximated by the following relation (5:29):

$$l_o \approx L_o / (R^{3/4})$$

where

R = Reynold's number

Since the atmosphere is dynamic, the sizes and number of these outer and inner scale variations are constantly changing. Thus, as the optical beam propagates through the atmosphere, the changes in the indices of refraction cause scintillations within the beam. To determine the "condition" of this received optical beam, these scintillations need to be predicted. Since they vary with time, statistical mathematical techniques must be used.

To describe the scintillations statistically, there are three parameters which must first be determined. They are: the probability distribution function of the intensity fluctuations, its mean, and its variance. These three quantities, as well as the refractive index structure constant and the power spectral density, will all need to be determined in order to predict the effects of turbulence on the optical beam.

The following sections will provide the necessary mathematical derivations for the determination of the aforementioned quantities.

The Refractive Index Structure Constant

The refractive index structure constant, denoted as C_n^2 , is a measure of how strong the index of refraction fluctuations are. Since these fluctuations are a function of temperature variations, then it would seem reasonable that C_n^2 must also vary with the temperature. In fact, it does!

Measurements (3:20-23) of C_n^2 have been made by using airborne mounted or balloon borne sensors which measure the temperature at various points in the atmosphere. This temperature data is then used to compute a temperature structure parameter, C_t^2 which is given (3:12-13) by

$$C_t^2 = r^{-2/3} E\{ [T(r_1) - T(r_2)]^2 \} \quad (2)$$

where

r = distance between r_1 and r_2
 $T(r_1), T(r_2)$ = temperature at either r_1 or r_2

Using the results from Eq. (2), C_n^2 can then be calculated
(3:13)

$$C_n^2 = [79 \times 10^{-6} (P/T^2)]^2 C_t^2 \quad (3)$$

where

P = pressure
T = temperature

By using Eq. (3), researchers could take experimental temperature data and compute numerical values for C_n^2 at a particular point in time. Data obtained from averaged C_n^2 measurements can be seen in Figure 3. The "hump" at 40,000 ft, in the figure, represents values of C_n^2 in the tropopause.

Using Figure 3, approximate values of C_n^2 may be calculated. By taking altitude intervals, and then fitting

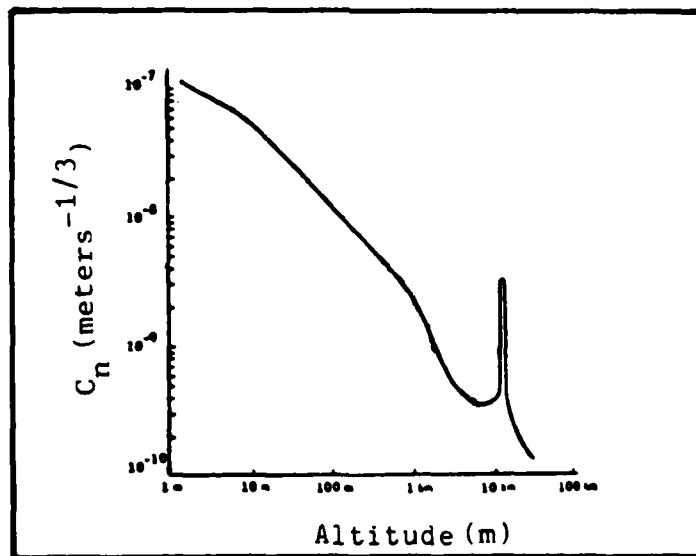


Figure 3. Experimental C_n^2 data (6:1960).

curves to the C_n data, the following expressions can be derived for determining C_n^2 .

10 m < altitude < 1 km :

$$C_n^2 = \left[\left[5.3 \times 10^{-8} - 5.07 \times 10^{-8} \left(\frac{\text{altitude}-10}{990} \right) \right] (4.642) \right]^2$$

1 km < altitude < 8 km :

$$C_n^2 = \left[\left[2.3 \times 10^{-9} - 1.97 \times 10^{-9} \left(\frac{\text{altitude}-1000}{7000} \right) \right] (4.642) \right]^2$$

8 km < altitude < 10 km :

$$C_n^2 = \left[\left[3.3 \times 10^{-10} - 3 \times 10^{-11} \left(\frac{\text{altitude}-8000}{1000} \right) + 3 \times 10^{-11} \left(\frac{\text{altitude}-8000}{1000} \right) \left(\frac{\text{altitude}-8000}{1000} - 1 \right) \right] (4.642) \right]^2$$

10 km < altitude < 14 km :

$$C_n^2 = \left[\left[3.3 \times 10^{-10} + 3.17 \times 10^{-9} \left(\frac{\text{altitude}-10000}{2000} \right) - 3.17 \times 10^{-9} \left(\frac{\text{altitude}-10000}{2000} \right) \left(\frac{\text{altitude}-10000}{2000} - 1 \right) \right] (4.642) \right]^2$$

Using the expressions above, different values for C_n^2 can be found by substituting the appropriate altitude into the appropriate expression. Figure 4 illustrates C_n^2 for a variety of altitudes.

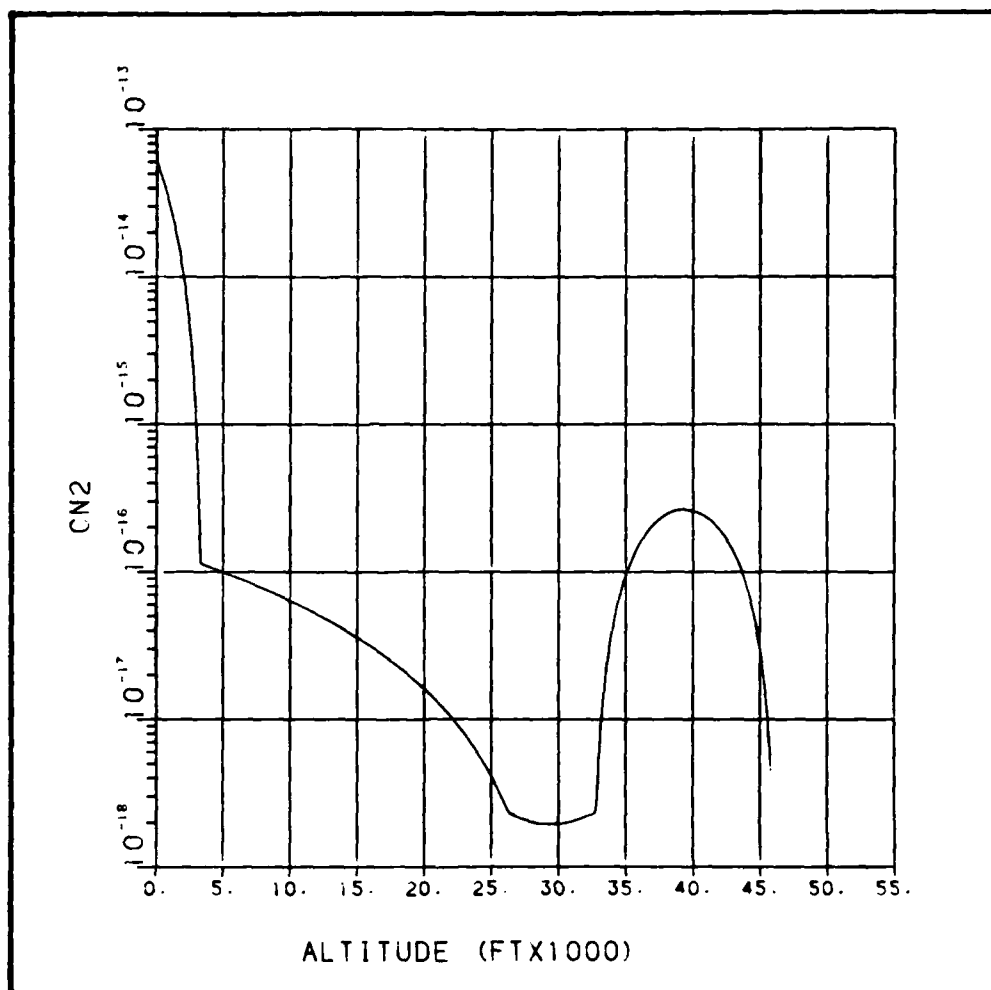


Figure 4. C_n^2 vs. altitude

Probability Distribution Function of the Intensity Fluctuations

The effects of atmospheric turbulence on an optical wave are unlike those of the corruptive noise. The effects due to turbulence are usually represented as multiplicative (7:1628); while those effects caused by noise are additive. A block diagram representing this convention is shown in

Figure 5. In communications theory, these multiplicative effects are more commonly referred to as time varying fading. Thus, as an optical beam propagates through the atmosphere, its intensity will fluctuate, or fade, with time.

Experimentation has shown that the intensity fluctuations of the optical beam appear to exhibit lognormal probability statistics. However, this is only true if the optical beam is not operating within the saturation region. A horizontal propagating beam is said to be in the saturation region when the following condition is satisfied:

$$k^{7/6} L^{11/6} C_n^2 > 5 \quad (4)$$

where

k = wavenumber

L = path length of the beam

Using this relation, Figure 6 illustrates the maximum propagation path length as a function of altitude. As long as this path length is below the curve, in Figure 6, then the optical beam is not considered to be in the saturation region.

While in the saturation region, there has been some doubt as to whether the statistics of the intensity fluctuations remain lognormal. In fact, there has been a great deal of research conducted which has attempted to determine what type of statistics are valid. Among some of the statistical distributions that have been considered are the Rayleigh, Rice-Nakagami, and K distributions.

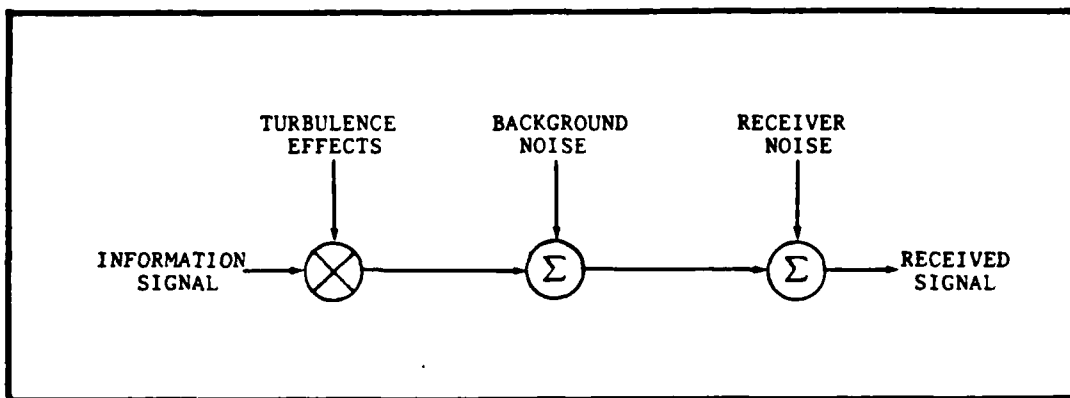


Figure 5. Communication system block diagram

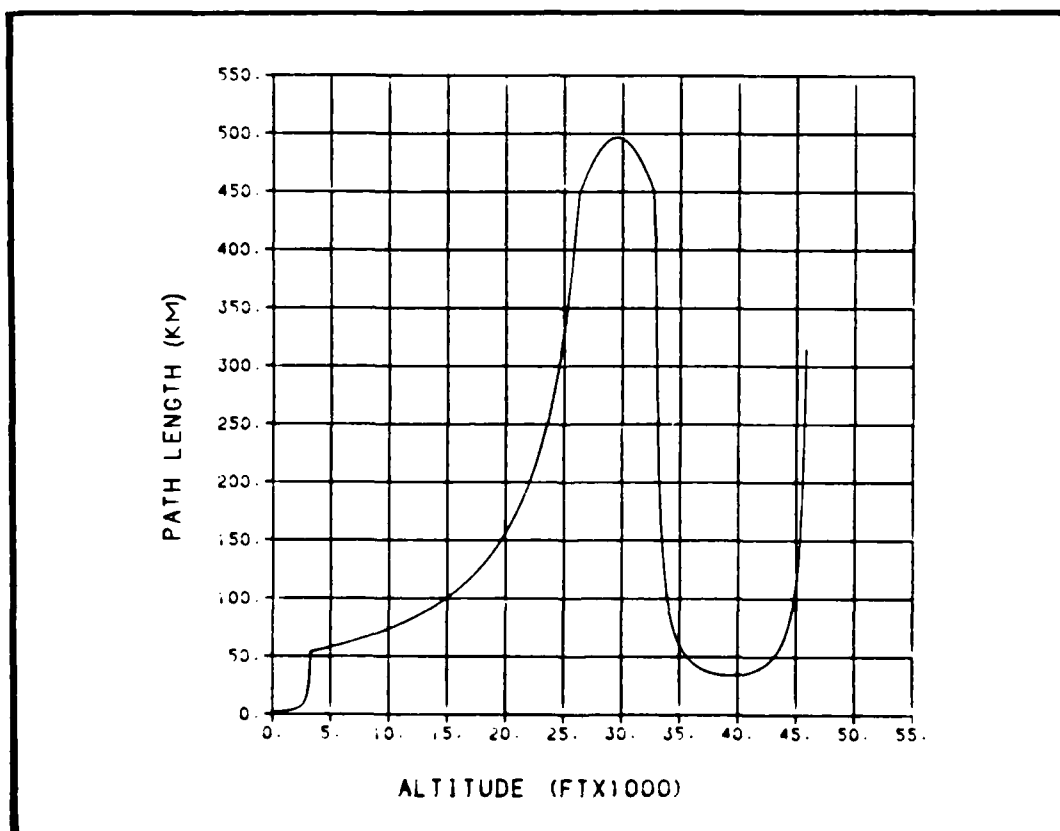


Figure 6. Maximum propagation path length of optical beam not in saturation

Since it has been shown that the probability distribution of the intensity fluctuations exhibits lognormal statistics, then all that needs to be determined are the parameters of this distribution, which are, its variance and its mean.

Derivation of the Variance and the Mean

The variance and the mean of the lognormal probability distribution can be found from using statistical mathematics in the following manner (8).

From elementary statistics, it is known that if a normal random variable (x) is written as

$$A = \exp(x)$$

then A is said to be lognormally distributed. Since the received field of the optical beam is distributed lognormally, then it can be represented as

$$U = U_0 \exp(x + j\theta)$$

where

U = field of the received beam
 U_0 = field of the transmitted beam
 x = log amplitude
 θ = phase

Then the intensity, I , of the received field is given by

$$\begin{aligned}
 I &= |U|^2 \\
 &= |U_0|^2 \exp(x + j\theta) \exp(x - j\theta) \\
 &= I_0 \exp(2x)
 \end{aligned} \tag{5}$$

Or, $I/I_0 = \exp(2x)$ (6)

If we take the natural log of both sides of Eq. (6), we get

$$\begin{aligned} \ln(I/I_0) &= \ln(\exp(2x)) \\ &= 2x \end{aligned} \quad (7)$$

But $\ln(I/I_0) = \ln(A^2/A_0^2)$

$$= 2\ln(A/A_0) \quad (8)$$

where

A = amplitude of the received wave
A₀ = amplitude of the transmitted wave

Combining Eqs. (7) and (8) we obtain

$$\begin{aligned} 2\ln(A/A_0) &= \ln(I/I_0) \\ &= 2x \end{aligned}$$

Or, $\ln(A/A_0) = x = \log \text{ amplitude}$

Since the normalized intensity, I/I_0 , is lognormally distributed, then the probability distribution function, $p(I/I_0)$ is given by

$$p(I/I_0) = \frac{1}{(I/I_0)\sqrt{2\pi}\sigma} \exp\left(-\frac{1}{2\sigma^2} (\ln(I/I_0) - E\{\ln(I/I_0)\})^2\right) \quad (9)$$

To determine σ^2 , observe that it is defined by

$$\sigma^2 = E\{\ln(I/I_0)^2\} - E^2\{\ln(I/I_0)\}$$

Using Eq. (7)

$$\begin{aligned} \sigma^2 &= E\{4x^2\} - E^2\{2x\} \\ &= 4E\{x^2\} - 4E^2\{x\} \\ &= 4[E\{x^2\} - E^2\{x\}] \end{aligned}$$

$$\sigma^2 = 4 \sigma_x^2 \quad (10)$$

Thus, the variance of the log intensity is equal to 4 times the variance of the log amplitude.

To determine the mean or $E\{\ln(I/I_0)\}$ in Eq. (9), the physical Law of Conservation of Energy must be used. In short, this means that the average amount of energy crossing the transmitter plane has to equal the total amount of energy crossing the receiver plane.

Thus

$$E\{|U_{rx}|^2\} = E\{|U_{tx}|^2\}$$

$$\text{Or,} \quad E\{I_{rx}\} = E\{I_{tx}\} \quad (11)$$

where

$$\begin{aligned} |U_{rx}|^2 &= I_{rx} = \text{intensity at the receiver} \\ |U_{tx}|^2 &= I_{tx} = \text{intensity at the transmitter} \end{aligned}$$

Taking the expected value of Eq. (5)

$$E\{I\} = E\{I_0\} E\{\exp(2x)\}$$

Dividing both sides by $E\{I_0\}$, and using Eq. (11)

$$1 = E\{\exp(2x)\}$$

$$E\{\exp(2x)\} = \int_{-\infty}^{\infty} \exp(2x) p(x) dx$$

Since x is normally distributed:

$$E\{\exp(2x)\} = \int_{-\infty}^{\infty} \exp(2x) \frac{1}{\sqrt{2\pi}\sigma_x} \exp \left(-\frac{(x - \bar{X})^2}{2\sigma_x^2} \right) dx$$

$$= \frac{1}{\sqrt{2\pi}\sigma_x} \exp\left(\frac{-\bar{X}^2}{2\sigma_x^2}\right) \int_{-\infty}^{\infty} \exp\left(\frac{-X^2}{2\sigma_x^2} + \left(2 + \frac{\bar{X}}{\sigma_x^2}\right)X\right) dX$$

Using the relation

$$\int_{-\infty}^{\infty} \exp(-ax^2 + bx) dx = \sqrt{\frac{\pi}{a}} \exp\left(\frac{b^2}{4a}\right)$$

The last equation above reduces to

$$\begin{aligned} E\{\exp(2X)\} &= \frac{1}{\sqrt{2\pi}\sigma_x} \exp\left(\frac{-\bar{X}^2}{2\sigma_x^2}\right) \sqrt{2\pi} \exp\left(\frac{\left(2 + \frac{\bar{X}}{\sigma_x^2}\right)^2}{2/\sigma_x^2}\right) \\ &= \exp\left(\frac{-\bar{X}^2}{2\sigma_x^2}\right) \exp\left[\left(\frac{\sigma_x^2}{2}\right)\left(4 + 4\frac{\bar{X}}{\sigma_x^2} + \frac{\bar{X}^2}{\sigma_x^4}\right)\right] \\ &= \exp(2\sigma_x^2 + 2\bar{X}) \end{aligned}$$

where

$$\bar{X} = E\{X\}$$

Thus

$$E\{\exp(2X)\} = \exp(2\sigma_x^2 + 2\bar{X})$$

Now

$$E\{\exp(2X)\} = \exp(2\sigma_x^2 + 2\bar{X}) = 1$$

Thus

$$\bar{X} = -\sigma_x^2 \quad (12)$$

$$E\{\ln(I/I_0)\} = E\{2X\}$$

$$= 2 E\{X\}$$

$$= -2\sigma_x^2 \quad (13)$$

Therefore, the revised probability distribution function of the intensity fluctuations can now be determined by

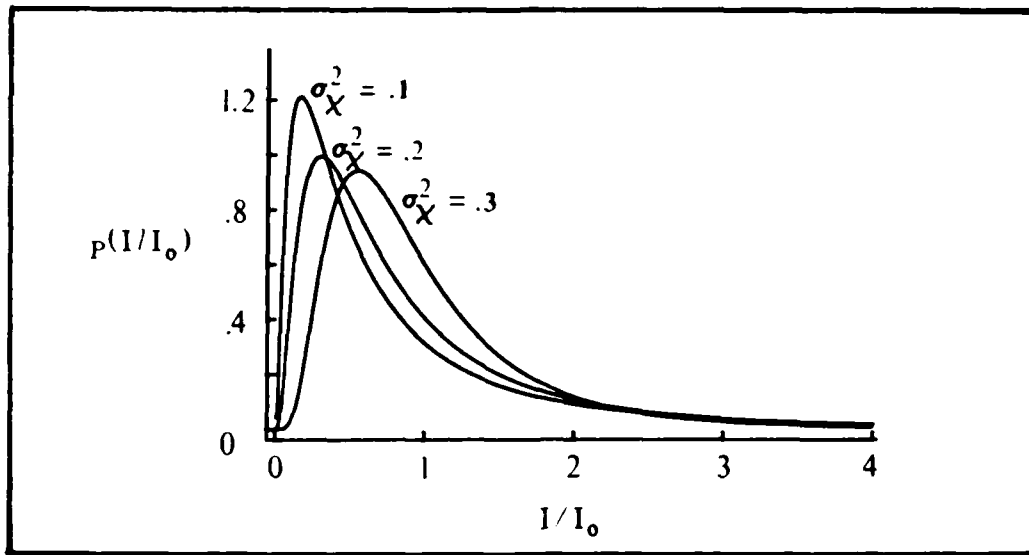


Figure 7. Lognormal distribution for a variety of σ_X^2 values.

substituting Eqs. (10), (12), and (13) into Eq. (9) to get

$$p(I/I_0) = \frac{1}{(I/I_0)\sqrt{8\pi}\sigma_X} \exp\left(-\left(\frac{\frac{1}{2}\ln(I/I_0) + \sigma_X^2}{2\sigma_X^2}\right)^2\right) \quad (14)$$

Figure 7 shows a plot of the probability density function $p(I/I_0)$ as a function of σ_X^2 .

As the inequality in Eq. (4) gets closer to 5, σ_X^2 increases to a value of approximately .64. However, when the beam "saturates" (condition in Eq. (4) is met), then σ_X^2 no longer increases. In fact, it has been noted that as either the path length or Cn^2 increases, there is a slight decrease in σ_X^2 . This phenomenon is illustrated in Figure 8.

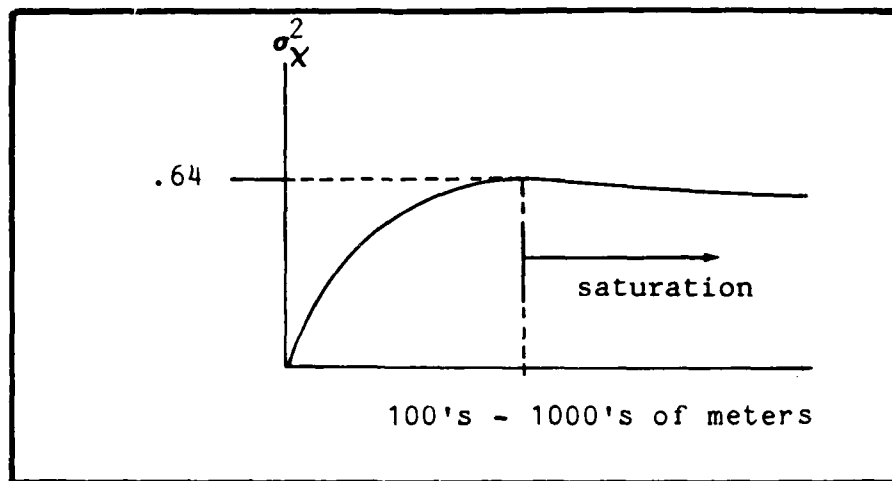


Figure 8. Phenomenon of decreasing variance in the saturation region.

Since the probability distribution function of Eq. (14) is a function of only one variable- σ_X^2 , then this parameter must be determined. In his works, Tatarski has shown that the variance of the log amplitude can be expressed (4:1534) as:

$$\sigma_X^2 = 2\pi^2 k^2 L \int_0^\infty \left[1 - \frac{k}{\gamma L} \sin\left(\frac{\gamma L}{k}\right) \right] \Phi(\gamma) \gamma d\gamma \quad (15)$$

where

k = wavenumber
 L = path length
 γ = spatial wavenumber ($2\pi/l$)
 l = scale size of an eddy
 $\Phi(\gamma)$ = power spectral density of the index of refraction fluctuations

However, Tatarski has also shown that if

$$l_0 \ll \sqrt{\lambda L} \quad (16)$$

where

l_0 = size of an inner scale variation

Then Eq. (15) can be approximated by

$$\sigma_x^2 = .124 C_n^2 k^{7/6} L^{11/6} \quad (17)$$

Since Eq. (16) is always true for reasonable path lengths (lengths greater than 10 meters), then Eq. (17) can be used with confidence.

Power Spectral Density

The frequency spectrum of the intensity fluctuations is known to be caused by the motion of the atmosphere. This motion can be separated into three groups:

- 1) Mean motion of the wind
- 2) Changes in the wind direction
- 3) Internal "mixing" motions of the atmosphere due to turbulence

Since this thesis is concerned with communications between two aircraft, then it will be assumed that the aircraft are stationary, and the atmosphere is moving rather than vice versa. If the "Frozen Turbulence Assumption" is used, then groups 2 and 3, above, may be neglected. This is due to the fact that the frozen turbulence assumption assumes that any variations in the indices of refraction, measured at a point, will be caused by the uniform motion of the atmosphere past that point. Thus, internal motion within the atmosphere may be neglected (4:1537). As a result, group 1 wind motions will be of primary interest. This

frozen turbulence assumption may only be used when $\sqrt{\lambda L} \ll L_0$, which is true most of the time.

Tatarski has noted that the "normalized" power spectral density ($U(f)$) of the intensity fluctuations can be written (5:218) as:

$$U(f) = \frac{f_0 W(f)}{\sigma_X^2} = 1.35 \Omega \int_0^{\infty} \left[1 - \frac{\sin(t^2 + \Omega^2)}{(t^2 + \Omega^2)} \right] (t^2 + \Omega^2)^{\frac{11}{6}} dt \quad (18)$$

where

$W(f)$ = true power spectral density
 Ω = f/f_0
 f_0 = $ws/\sqrt{2\pi\lambda L}$
 ws = wind speed

Typically, most literature represents the normalized power spectral density as shown in Figure 9. However, by rewriting the axes, a "denormalized" version of Figure 9 can be found.

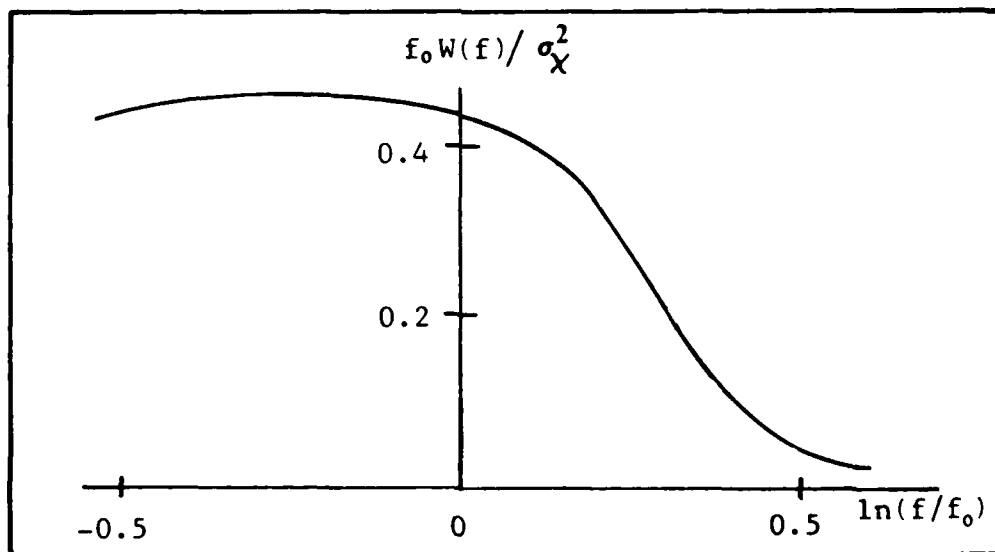


Figure 9. Normalized power spectral density of the intensity fluctuations (5:218).

Development of the Denormalized Power Spectral Density

Before the denormalized version of the power spectral density of Figure 9 can be determined, values for $f_0 W(f) / \sigma_x^2$ vs. the corresponding values for $\log(f/f_0)$ must be found. This can be done by directly reading them from Figure 9. For example, when $\frac{f_0 W(f)}{\sigma_x^2} = .43$, then

$$\log(f/f_0) = 0 \quad (19)$$

Thus,

$$f = f_0 = \frac{ws}{\sqrt{2\pi\lambda L}} \quad (20)$$

Since Figure 9 was based on $ws = 1\text{m/s}$, $L = 1000\text{m}$, and $\lambda = 5121 \text{ \AA}$ then

$$f = f_0 = \frac{1}{\sqrt{2\pi(5121 \times 10^{-10})(1 \times 10^3)}} = 17.63 \text{ Hz}$$

Finally, to determine that value of $W(f)$ (denormalized power spectral density value) which corresponds to $f_0 = 17.63 \text{ Hz}$, σ_x^2 needs to be calculated. To do this, C_n^2 must first be determined from the available parameters- namely the altitude. By using the relations derived earlier, C_n^2 can be calculated. Once C_n^2 has been determined, σ_x^2 is found from Eq. (17).

From here on, $W(f)$ can be found for any value of frequency in the power spectral density by reading Figure 9 and transforming them as shown above. An example of a denormalized power spectral density is shown in Figure 10. As can be seen, Figure 10 actually resembles a Chebychev low

pass filter. As will be seen in Chapter III, this fact will be useful in modeling the power spectral density.

Summary

In summary, it has been determined that the intensity fluctuations of the optical beam exhibit lognormal statistics, and are a function of many parameters. To model these fluctuations, the following expressions have been derived

$$E\{X\} = -\sigma_X^2$$

$$\sigma_X^2 = .124 C_n^2 k^{7/6} L^{11/6}$$

$$p(I/I_0) = \frac{1}{(I/I_0)\sqrt{8\pi}\sigma_X} \exp\left(-\frac{(\frac{1}{2}\ln(I/I_0) + \sigma_X^2)^2}{2\sigma_X^2}\right)$$

In addition, a means of representing the power spectral density of the intensity fluctuations has been developed, which in turn will be used as a basis for the computer simulation.

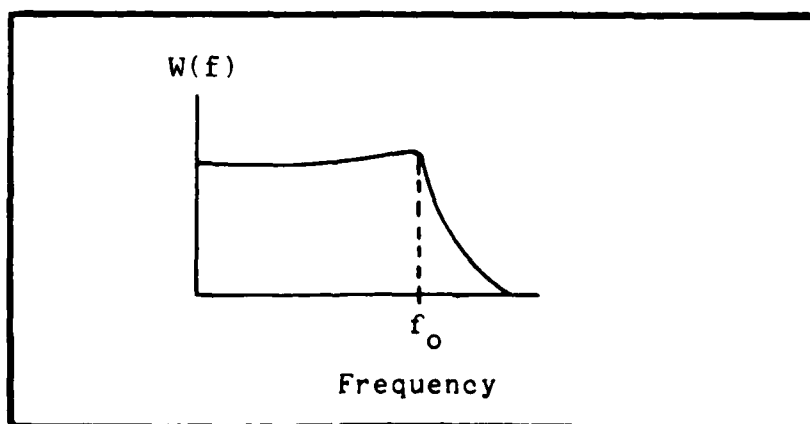


Figure 10. Denormalized power spectral density.

III. Mathematical Derivation of the Simulation

Introduction

In Chapter II, the intensity fluctuations of the optical wave were found to be distributed lognormally. It was also determined that these scintillations affected the beam in a multiplicative manner rather than in an additive one. To represent this convention, the model shown in Figure 11 will be used as a basis for this thesis. To determine how reliable this communication system will be, each of the factors shown in Figure 11 must be modeled mathematically.

The ultimate goal of this simulation will be to transmit a binary digital signal, $s(n)$, through the atmospheric channel and into the receiver. While in the receiver, the received signal sequence, $r(n)$,

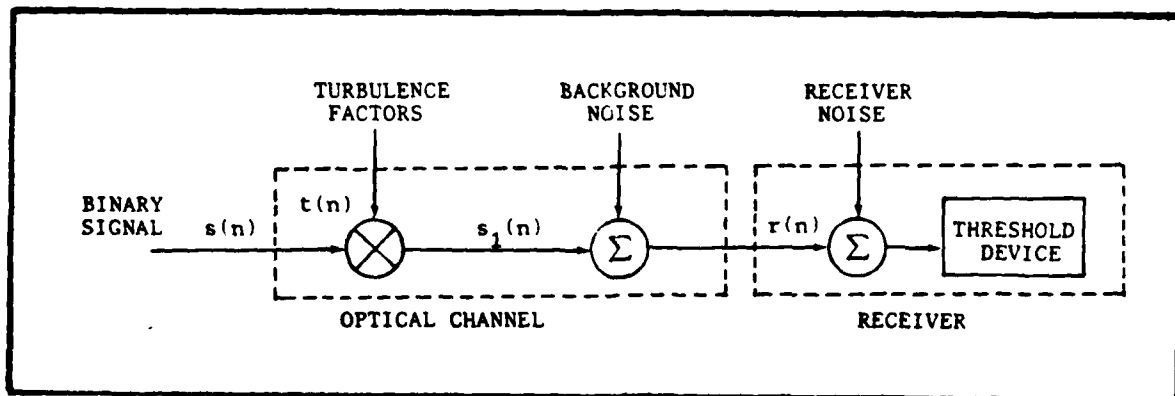


Figure 11. Communication system model.

will be corrupted by noise and then processed. The receiver will use a threshold detection technique to determine whether a 1 or a 0 was transmitted. By comparing what was sent to what the receiver decided was sent, a bit error rate can be established. Running this simulation with varying environmental conditions (i.e. altitude, propagation path length, and aircraft speed) should give a good indication of the effects of turbulence and noise on an air-to-air optical communication link.

The ensuing sections of this chapter will present the method and approach used to model each of the elements shown in Figure 11. Once modeled, the complete simulation can be run and the bit error rate determined.

Simulation of the Input Signal

Since we are dealing with a digital communication scheme (on/off keying), the input signal can be represented as a random sequence of 1's and 0's being transmitted through the optical channel.

Using the International Mathematical and Statistical Library (IMSL) subroutines, pseudorandom numbers between 0 and 1, can be generated. Once generated, these numbers can be transformed into binary 1's and 0's using the following logic scheme

Let: x = IMSL pseudorandom number
 y = binary signal bit

If: $x \geq .5$ then $y = 1$
 $x < .5$ then $y = 0$

By repeatedly doing this (about 750,000 times per simulation run), an information signal sequence containing 750,000 1's and 0's can be transmitted through the optical channel.

Simulation of the Atmospheric Channel

From the communication block diagram, the optical channel is shown to consist of two elements: atmospheric turbulence, and background noise. Each of these elements are random processes and, as such, must be dealt with using statistical mathematics.

Using Figure 11 as a reference, the modeling goal for the optical channel will be to develop a sequence of numbers, $t(n)$, which can be multiplied by the signal sequence, $s(n)$. The multiplicative product, $s_1(n)$, will represent the corrupted signal sequence. The intensity of each bit in $s_1(n)$ must fluctuate lognormally. Once this sequence is produced, it can then be corrupted by noise from any background radiation present at the time.

As mentioned earlier, various researchers have shown that based upon theoretical and experimental considerations the intensity fluctuations of the optical signal exhibit lognormal statistics. However, when these researchers have turned to experimental methods, the optical beams used have always consisted of a constant intensity. To grasp the approach taken in this thesis for modeling the scintillation effects, an analogy between a real experiment and an

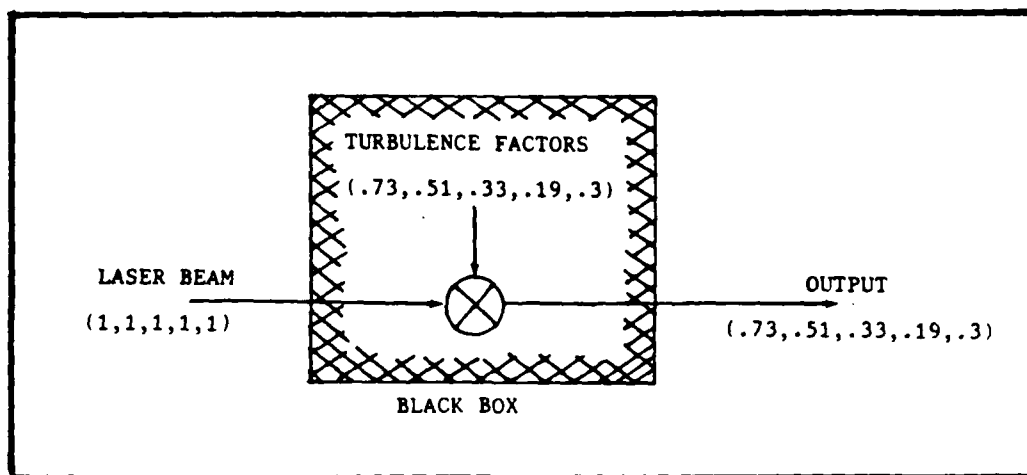


Figure 12. Black box analogy.

illustrative example can be drawn.

This analogy is illustrated in Figure 12. Here a "digital" laser beam of constant intensity is passed through a "black box." Let the term "constant intensity" mean a continuous stream of digital 1's. As this beam passes through the box, its intensity gets "multiplied" by some other sequence of numbers (call them turbulence factors). Assume that these turbulence factors fluctuate lognormally and have a power spectral density resembling the frequency response of a low pass filter. As the beams exits, its intensity is no longer constant. Instead, it fluctuates lognormally and has a low pass filter-like power spectral density. Since its intensity, entering the box, was constant (i.e. a sequence of digital 1's), then the sequence of

bits coming out of the box must be equal to the multiplicative turbulence factor sequence of bits in the box.

Therefore, we can model a turbulence influenced optical beam using the black box analogy. This means that the turbulence element, $t(n)$ in Figure 11, can be modeled as a random sequence of numbers whose magnitude fluctuates lognormally and power spectral density (PSD) resembles a Chebychev-like low pass filter. This sequence of numbers will then be multiplied by the signal $s(n)$. To generate a random series of numbers to meet these requirements, a technique developed by Gujar and Kavanaugh (9:716-719) can be used.

The principle behind this technique is illustrated in Figure 13. A random signal, $x(t)$, has a gaussian distribution, $p_x(x)$, and a known PSD, $S_x(\omega)$. The transfer

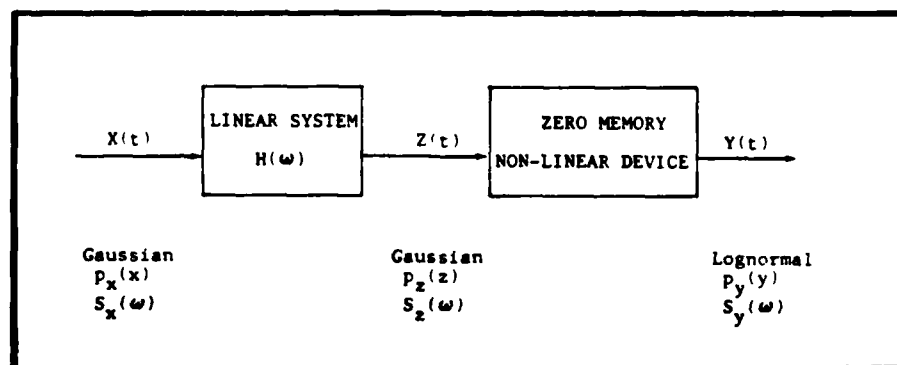


Figure 13. Block diagram of the Gujar Kavanaugh technique (10:17).

function, $H(\omega)$, of the linear filter is chosen such that it will produce an output signal, $z(t)$, which is also gaussian but has the desired PSD. The signal, $z(t)$, is then passed through a non-linear device. The resulting signal, $y(t)$, will have both the desired probability distribution and PSD.

The desired transfer function, $H(\omega)$, can be determined from elementary stochastic theory in the following manner

$$\begin{aligned}
 \text{If:} \quad & S_x(\omega) = \text{PSD of the input signal} \\
 & S_z(\omega) = \text{PSD of the output signal} \\
 & H(\omega) = \text{filter transfer function} \\
 \text{Then:} \quad & S_z(\omega) = |H(\omega)|^2 S_x(\omega) \\
 \text{If:} \quad & S_x(\omega) \text{ is white} \\
 \text{Then:} \quad & S_x(\omega) = 1 \\
 & S_z(\omega) = |H(\omega)|^2 \\
 & H(\omega) = \sqrt{S_z(\omega)} \quad (1)
 \end{aligned}$$

This means that the magnitude squared of the filter's transfer function is equal to the desired PSD.

To duplicate the above technique for the computer simulation, the input signal, $x(t)$, must have a gaussian distribution and a white PSD. This input signal can be generated from the IMSL computer subroutines. Since the gaussian random variables are generated from a uniform distribution, they should inherently have a white PSD.

Also, since the signal being passed through the linear filter is digital, then this linear filter must also be digital. This means that its transfer function must be

represented in the Z domain. To do this, the transfer function must first be characterized in the analog domain and then transformed into the Z domain. To describe the analog filter transfer function the proper filter coefficients must be found. Since the desired PSD of the intensity fluctuations, $S_z(\omega)$, resembles a Chebychev filter, then, from Eq. (1) the filter transfer function must also resemble a Chebychev filter. To properly characterize this filter, its order, cut-off and passband attenuation magnitudes must be specified.

The order of the filter determines how sharp the roll off rate will be in its transition band. The higher the order, the sharper the roll off. By knowing the various cutoff frequency and attenuation specifications, the filter order can be computed. To determine the order, the following relation (10:90) can be used

$$n = \frac{\cosh^{-1} \left((10^{0.1A_{\min}} - 1) / (10^{0.1A_{\max}} - 1) \right)^{\frac{1}{2}}}{\cosh^{-1} (\omega_s / \omega_c)}$$

where

n = order of the filter
 A_{\min} = attenuation (dB) of frequencies in the stopband
 A_{\max} = magnitude (dB) of ripple in the passband
 ω_s = frequency at A_{\min}
 ω_c = maximum frequency which will pass through the filter with a minimum of attenuation

A_{\max} and A_{\min} are constants, while ω_s and ω_c are variables which are functions of the altitude, propagation path

Table II

Chebyshev filter orders for a variety of optical propagation environments.

Aircraft Speed (knts)	Altitude (ft)	Propagation Path Length (m)	Filter Order
300	25,000	80,000	2.9639
350	30,000	50,000	2.9861
400	30,000	50,000	2.9473
450	30,000	75,000	2.9178

length, and aircraft speed. Table II presents a few values of n for a variety of environmental parameters. As can be seen, the next highest integer value under the heading "Filter Order" is 3. Therefore, the order of this linear filter can be approximated to be 3.

A normalized 3rd order analog Chebyshev filter will always have a transfer function as follows

$$H(s) = \frac{1}{s^3 + 1.6293s^2 + 2.0773s + 1.1516} \quad (2)$$

To convert this normalized filter transfer function into any desired filter transfer function, the variable s , in Eq. (2), must be divided by the frequency at the desired filter's 3dB point. The result is

$$H(s) = \frac{1}{(s/\omega)^3 + 1.6293(s/\omega)^2 + 2.0773(s/\omega) + 1.1516} \quad (3)$$

where

$\omega = 3$ dB bandwidth

Thus, Eq. (3) is the transfer function of the desired analog filter.

The transformation from the analog to the digital domain is not a difficult one. This conversion can be done by using the bilinear transformation technique. To obtain $H(z)$, the following substitution must be made into Eq. (3)

$$\text{Let} \quad s = \frac{2(z-1)}{t(z+1)} \quad (4)$$

where

$t =$ sampling time

The result of this substitution is

$$H(z) = \frac{1}{\left(\frac{2(z-1)}{t\omega(z+1)}\right)^3 + 1.6293\left(\frac{2(z-1)}{t\omega(z+1)}\right)^2 + 2.0773\left(\frac{2(z-1)}{t\omega(z+1)}\right) + 1.1516} \quad (5)$$

Substituting Eq. (4) into Eq. (3), however, does result in a distortion of the frequency axis. To compensate for this distortion, the 3 dB frequency term present in Eq. (5) must be warped. Using the following substitution, this distortion can be minimized. Let

$$\omega = \frac{2}{t} \tan^{-1}(\omega_0 t/2) \quad (6)$$

where

$t =$ sampling time

$\omega_0 =$ frequency at 3 dB point of the digital filter

By substituting the results of Eq. (6) into Eq. (5), the desired digital filter transfer function can be written as

$$H(z) = \frac{1}{\left(\frac{2(z-1)}{t\omega_0(z+1)}\right)^3 + 1.6293\left(\frac{2(z-1)}{t\omega_0(z+1)}\right)^2 + 2.0773\left(\frac{2(z-1)}{t\omega_0(z+1)}\right) + 1.1516} \quad (7)$$

Multiplying the numerator and denominator of Eq. (7) by $(t\omega_0/2)(z+1)^3$, Eq. (7) becomes

$$H(z) = \frac{\left(\frac{t\omega_0(z+1)}{2}\right)^3}{(z-1)^3 + 1.6293\frac{(t\omega_0(z+1))}{2}(z-1)^2 + 2.0773\frac{(t\omega_0(z+1))^2}{4}(z-1) + 1.1516\frac{(t\omega_0(z+1))^3}{8}} \quad (8)$$

Expanding and rewriting Eq. (8)

$$H(z) = \frac{A(z^3 + 3z^2 + 3z + 1)}{(z^3 - 3z^2 + 3z - 1) + B(z^3 - z^2 - z + 1) + C(z^3 + z^2 - z - 1) + D(z^3 + 3z^2 + 3z + 1)} \quad (9)$$

where

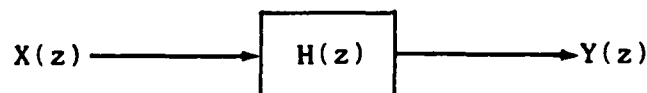
$$A = \left(\frac{t\omega_0}{2}\right)^3$$

$$B = 1.6293\left(\frac{t\omega_0}{2}\right)$$

$$C = 2.0773\left(\frac{t\omega_0}{2}\right)^2$$

$$D = 1.1516\left(\frac{t\omega_0}{2}\right)^3$$

Since this is a linear system, then



Where

$$Z(z) = H(z) X(z)$$

Thus

$$H(z) = \frac{Z(z)}{X(z)} = \frac{Az^3 + 3Az^2 + 3Az + A}{(1+B+C+D)z^3 + (C-3-B+3D)z^2 + (3-B-C-3D)z + (B-1-C+D)}$$

Multiplying by $1, \left(\frac{z^{-3}}{z^{-3}}\right)$, and rewriting

$$\begin{aligned} Z(z) & \left[(1+B+C+D) + (C-3-B+3D)z^{-1} + (3-B-C-3D)z^{-2} + (B-1-C+D)z^{-3} \right] \\ & = X(z) \left[A + 3Az^{-1} + 3Az^{-2} + Az^{-3} \right] \end{aligned} \quad (10)$$

Taking the inverse Z transform, Eq. (10) may be written as:

$$\begin{aligned} z(n) = \frac{1}{1+B+C+D} & \left[Ax(n) + 3Ax(n-1) + 3Ax(n-2) + Ax(n-3) \right. \\ & - (C-3-B+3D)z(n-1) - (3-B-C-3D)z(n-2) \\ & \left. - (B-1-C+D)z(n-3) \right] \end{aligned} \quad (11)$$

Equation (11) is written in a form which lends itself extremely well to computer simulation. As can be seen, $z(n)$ is a function of past and present inputs as well as past outputs. Since $z(n)$ is a series of random variables, they have a set of statistics associated with them. Also, since the random variables in $x(n)$ are zero mean gaussian random variables, and the transformation is linear; then $z(n)$ must also be a sequence of zero mean gaussian random variables. However, its variance will not be the same as that of $x(n)$. Instead it will be

$$\sigma_y^2 = \frac{1}{\alpha-1} \sum_{n=0}^{\alpha} [y(n)]^2 \quad (12)$$

In addition, the PSD of $z(n)$ will not be white. Since the filter transfer function is equal to the square root of $S_z(\omega)$, then from Eq. (1), $z(n)$ should have the power spectrum of the intensity fluctuations.

The nonlinear device shown in Figure 13 must now be specified. According to Gujar and Kavanaugh, this nonlinear device is really a one-to-one transformation between z and y . Consequently, for any point (z,y) in the transformation, the probability of z being in the range $z-\delta z$ to z is equal to the probability that y is in the corresponding range of $y-\delta y$ to y . That is

$$p_z(z-\delta z/2) |\delta z| = p_y(y-\delta y/2) |\delta y| \quad (13)$$

Since the probability distributions of z and y are known, then the only variables which need to be evaluated are δz and δy . To solve for these parameters, a small value is assigned to δz . For example, let $\delta z = .0001$. To determine the corresponding δy , an initial z and y value must be chosen such that

$$P_z(Z \leq z) \approx P_y(Y \leq y) \quad (14)$$

Initial values of z and y are chosen such that the upper limits (i.e. $P_z(Z \leq z) = P_y(Y \leq y) = .999$) of Eq. (14) are met. Once these values for z and y , and $\delta x = .0001$ are substituted into Eq. (11), δy can be determined. Once δy is calculated, then for any value of z , the corresponding value

of y can be found. Thus, the output sequence, $y(n)$, will have a lognormal distribution.

This $y(n)$ sequence is then designated as $t(n)$ and is shown in Figure 10. As shown, it will be multiplied by the binary signal, $s(n)$, and form a new signal $s_1(n)$ which will have an intensity which fluctuates lognormally. It should be noted that there cannot be a one-to-one multiplication between $t(n)$ and $s(n)$. $S(n)$ is being transmitted at a rate of 20,000 bits per second (or 1 bit every .05 msec), while the "transmission" of the turbulence factors, $t(n)$, depends on the sampling time. Typically, this sampling time is greater than .05 msec. This means that the same turbulent factor number, $t(n)$, might be multiplied by more than one signal bit. For the purposes of this simulation, the number of information bits that will be multiplied, must be an integer value (bit splitting will not be permitted). For this to occur, the digital sampling time must be such that when multiplied by the bit rate, an integer product will result. For example, assume that the digital sampling time is: $t = .14$ msec, then

$$20,000 \text{ bps} \times .14 \text{ msec} = 2.8 \quad (15)$$

Since 2.8 is not an integer, then the sampling time must be increased so that the next highest integer, 3, is obtained in Eq. (15). To obtain this value, the new sampling time must be

$$\begin{aligned} t &= 3/20,000 \text{ bps} \\ &= .15 \text{ msec} \end{aligned}$$

Thus, for every turbulent factor produced, it will be multiplied by 3 consecutive signal bits.

To determine if the Gujar Kavanaugh method does indeed produce the desired PSD at the output of the non-linear device, the Fast Fourier Transform (FFT) can be used. By taking the FFT of each sequence, $z(n)$ and $y(n)$, and then comparing them; a determination can be made as to their similarity. Figure 14 illustrates the FFT for a sample sequence. Note that the PSD of the sample digital sequence repeats itself every 2000 Hz. This is because the sampling time is .5 msec, or 1/2000 Hz. From this figure, it can be seen that one PSD is indeed a scaled version of the other, and both have identical frequency components. Therefore, it can be concluded that the Gujar Kavanaugh method will work for this simulation.

Background Radiation

For the purposes of this thesis, it will be assumed that the major source of background radiation will be due to the sunlit sky. Typically, the strength of the background radiation is described in terms of its spectral radiance, $N(\lambda)$. The spectral radiance can be defined as: the radiant power in a solid angle per unit projected area of a source on a hemisphere (11:113). Accurate values for $N(\lambda)$ cannot

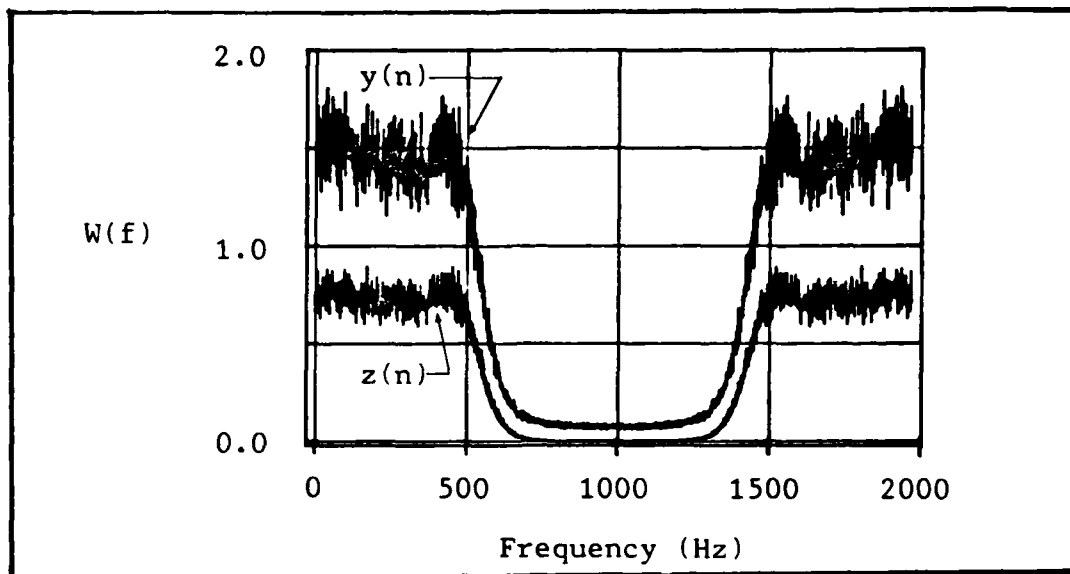


Figure 14. FFT of the sequences $z(n)$ and $y(n)$.

usually be computed from a general mathematical expression. Instead, they must be measured experimentally. This should make sense since $N(\lambda)$ is a function of many environmental parameters such as altitude, cloud cover, temperature, and source-receiver geometry. For the purpose of this thesis, $N(\lambda)$ will be chosen such that it represents somewhat of a worst case condition. Once $N(\lambda)$ has been chosen, then the average background radiation power can be computed (11:118) from

$$P_b = \tau_r N(\lambda) \Omega B A_r$$

where

τ_r = receiver optics transmissivity

Ω = field of view (steradians)

B = Optical bandwidth (\AA)

A_r = area of receiver aperture (m^2)

For the optical communication link used in this thesis:

$$N(\lambda) = .015 \text{ W}/(\text{m}^2 \text{ sr } \text{\AA})$$

$$\tau_r = .8$$

$$\begin{aligned}\Omega &= 3.848 \times 10^{-5} \text{ sr} \\ A_r &= 1.2667 \times 10^{-2} \text{ m}^2 \\ B &= 100 \text{ A}\end{aligned}$$

Therefore

$$\begin{aligned}P_b &= (.8)(.015)(3.848 \times 10^{-5})(100)(1.2667 \times 10^{-2}) \\ &= 5.85 \times 10^{-7} \text{ Watts}\end{aligned}$$

This value represents the total amount of power impinging on the detector in the absence of any information signal.

Optical Beam Divergence

As the beam transmission path increases, the optical beam begins to diverge. Divergence can be defined as the spreading of an optical beam as its propagation path increases. As a result, the amount of power, in the receiver plane, is smeared over an area much larger than that of the transmitter aperture. From Figure 15, it can be seen that the amount of power received (P_r), is proportional to the power collected over the total power present in the receiver plane.

This relationship can be written as

$$P_r = P_t \tau_a \tau_t \tau_r \frac{A_{rx}}{\Omega^2 L^2} \quad (19)$$

where

P_t = transmitter power
 A_{rx} = area of receiver
 L = propagation path length
 τ_a = atmospheric transmissivity
 τ_r = receiver transmissivity
 τ_t = transmitter transmissivity
 Ω = field of view

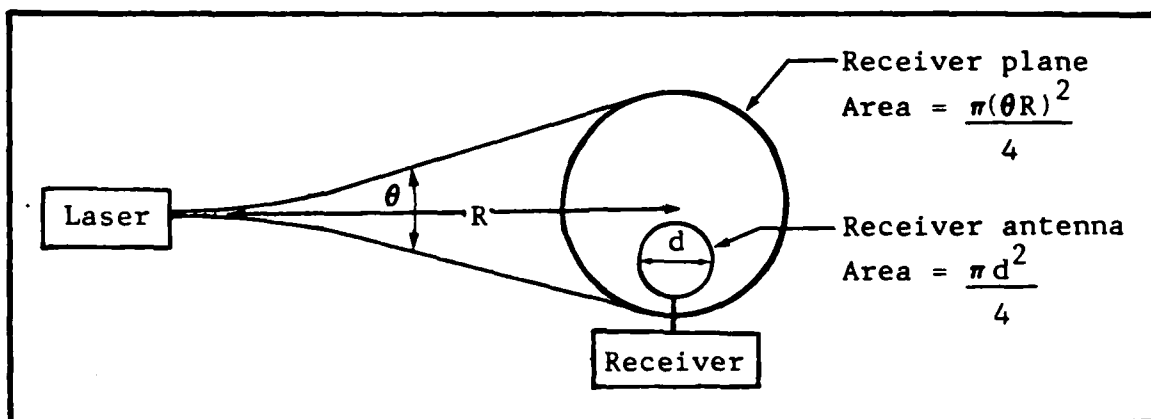


Figure 15. Divergence of the optical beam as the propagation path length increases.

The transmissivity factors present in Eq. (19) represent the efficiency of transmission through the desired medium. The atmospheric transmissivity factor (τ_a) determines the amount of power which is able to pass through the atmosphere unattenuated. This factor can be written (12:61) as follows

$$\tau_a = \exp(-\alpha_a \beta L) \quad (20)$$

where

α_a = extinction coefficient
 β = aerosol scaling factor
 L = propagation path length (km)

From LOWTRAN 5 computer simulation plots (12:24,31), the extinction coefficient and aerosol scaling factors can be written as follows:

For $\lambda = .904 \text{ m}$ $\alpha_a = .45$,

$0 \leq \text{altitude} < 4 \text{ km}$:

$$\beta = .2 - .19 \left(\frac{\text{altitude}}{4000} \right) \quad (21)$$

4 km \leq altitude < 7 km:

$$\beta = .01 - .004 \left(\frac{\text{altitude} - 4000}{3000} \right) \quad (22)$$

7 km \leq altitude \leq 16 km:

$$\beta = .006 - .0056 \left(\frac{\text{altitude} - 7000}{9000} \right) + .0056 \left(\frac{\text{altitude} - 7000}{9000} \right) \left(\frac{\text{altitude} - 7000}{9000} - 1 \right) \quad (23)$$

As can be seen above, the aerosol scaling coefficient is a function of the altitude. The transmitter and receiver transmissivity factors describe the percentage of the optical signal power which is passed through both the transmitter and receiver, respectively.

Simulation of the Receiver

Once the corrupted signal's field is incident upon the photodetector, an electrical current is produced. While passing through the receiver, this current undergoes additional corruptive effects (i.e. dark current, shot and thermal noise). This signal is then fed into a decision making device called a threshold detector. The threshold detector compares the level of the signal with a predetermined threshold value. If the signal is equal to or greater than this threshold value, then the receiver decides that a 1 was transmitted; otherwise, a decision is made that a 0 was sent.

Before developing the mathematical model for this type of receiver, the following photodetector design criteria will be assumed:

- 1) The detector will be thermal noise limited.
- 2) A DC current block will be used.
- 3) The load resistance (R_L) will be equal to 30 ohms.
- 4) The receiver has an internal gain of 40.

Since the dark current is strictly DC, the DC current block filters it out from the average current. Therefore, for the purpose of this simulation, its effects can be neglected.

but, there are two other types of noise which must also be dealt with. They are, the shot noise and the thermal noise. If we assume that the photodetector is thermal noise limited, then we can overlook the shot noise due to the photodetector. However, we cannot ignore the shot noise due to the constant background radiation.

Typically, both the thermal and background noise manifest themselves as unwanted current components. These extraneous currents can be modeled as random variables which get added directly to the received signal current. Characteristically, the thermal noise current can be modeled as a zero mean gaussian random variable, while the background noise current has been found to exhibit Poisson characteristics. If we assume that the background noise level is quite high, such as daylight conditions, then it

can be assumed that the background noise can also be modeled as a gaussian random variable (2:222-224).

Since both processes have a zero mean, then their variances are directly proportional to there respective PSD's. In fact, their variances are equal to their respective power levels. Also, because of the fact that we are using avalanche photodetectors (APD's), the variances may be written as follows:

For thermal noise,

$$\sigma_t^2 = \frac{(2)(B)(2kT)}{R_1}$$

where

B = electrical bandwidth
 k = Boltzmann's constant
 T = temperature °K
 R₁ = load resistance

For the background radiation,

$$\sigma_b^2 = \frac{(2)(B)(\eta P_b q^2 G^{2+.3})}{h f}$$

where

B = electrical bandwidth
 η = efficiency
 P_b = power of background radiation
 q_b = charge of electron
 G = gain
 h = Planck's constant
 f = frequency of light

Using the parameters of the communication system, the respective variances are

$$\sigma_b^2 = \frac{(2)(5 \times 10^6)(2)(1.38 \times 10^{-23})(300)}{30}$$

$$= 2.76 \times 10^{-15}$$

$$\sigma_t^2 = \frac{(2)(5 \times 10^6)(.85)(5.85 \times 10^{-7})(1.6 \times 10^{-19})(40^{2.3})}{(6.62 \times 10^{-34})(3.31 \times 10^{14})}$$

$$= 2.804 \times 10^{-15}$$

Now, by using the IMSL routines, these normal $(0, 2.76 \times 10^{-15})$ and normal $(0, 2.804 \times 10^{-15})$ random variables can be generated and then added to the signal current. The resulting signal is then passed through the threshold device.

The threshold value for this device must be chosen such that the probability of making an incorrect decision is minimized.

Determination of the Threshold Level

In order to determine the effects of atmospheric turbulence on an optical signal, a "baseline" system must first be developed. The design of this baseline system will consist of a communication link which does not take into account the effects of turbulence. By comparing a turbulence corrupted signal with a signal from this baseline system, a comparison can be drawn. This comparison will enable us to determine how the bit error rate is affected by turbulence.

Since we are simulating an on/off keying communication system, then the only two possible hypothesis m_1 and m_2 corresponding to the signals entering the decision device are

$$m_1 : s = B + T \quad (24)$$

$$m_2 : s = \mu + B + T \quad (25)$$

where

T = random thermal noise current
 B = random background radiation current
 μ = average signal current

Since both T and B are zero mean gaussian random variables

Let

$$X = B + T$$

Where

$$E\{X\} = 0$$

$$E\{X^2\} = \sigma_b^2 + \sigma_t^2$$

Therefore

$$\begin{aligned} \sigma_x^2 &= 2.804 \times 10^{-15} + 2.76 \times 10^{-15} \\ &= 5.564 \times 10^{-15} \end{aligned}$$

This allows Eqs. (24) and (25) to be rewritten as

$$m_1 : s = X \quad (26)$$

$$m_2 : s = \mu + X \quad (27)$$

Now

$$p(s|m_1) = p_x(X)$$

$$p(s|m_2) = p_x(X - \mu)$$

Since the probability distribution of X is gaussian, we get

$$p_x(x) = \frac{1}{\sqrt{2\pi}\sigma_x} \exp\left(-\frac{1}{2\sigma_x^2}(x)^2\right) \quad (28)$$

$$p_x(x - \mu) = \frac{1}{\sqrt{2\pi}\sigma_x} \exp\left(-\frac{1}{2\sigma_x^2}(x - \mu)^2\right) \quad (29)$$

The system probability of error, P_e , can be written as

$$P_e = P(\text{deciding a 1} \mid 0 \text{ sent}) P(0) + \\ P(\text{deciding a 0} \mid 1 \text{ sent}) P(1)$$

Let $P(0) = P(1) = \frac{1}{2}$

Then

$$P_e = \frac{1}{2} \left(P(\text{deciding a 1} \mid 0 \text{ sent}) + \right. \\ \left. P(\text{deciding a 0} \mid 1 \text{ sent}) \right) \\ = \frac{1}{2} \left(\frac{1}{\sqrt{2\pi}\sigma_x} \int_k^{\infty} \exp\left(-\frac{1}{2\sigma_x^2}(x)^2\right) dx + \frac{1}{\sqrt{2\pi}\sigma_x} \int_{-\infty}^k \exp\left(-\frac{1}{2\sigma_x^2}(x - \mu)^2\right) dx \right) \quad (30)$$

where

k = threshold value

The optimum threshold (11:169) value for this type of system would be

$$k = \left(\frac{\mu}{2}\right) + \left(\frac{\sigma_x^2}{\mu}\right) \ln\left(\frac{P(0)}{P(1)}\right) \\ k = \frac{\mu}{2} \quad (31)$$

where

μ = average current due to the signal
and the background radiation

Before a threshold value can be assigned, an optimum value of the system probability of error must be designated. Due to the constraints of computer time, P_e for this system must be at least 10^{-5} .

Substituting Eq. (31) into Eq. (30) and rewriting gives

$$\begin{aligned} 10^{-5} &= \frac{1}{2} \left(Q\left(\frac{k}{\sigma_x}\right) + Q\left(\frac{\mu - k}{\sigma_x}\right) \right) \\ 10^{-5} &= Q\left(\frac{\mu}{2\sigma_x}\right) \end{aligned} \quad (32)$$

If, for example

$$Q(x) = 10^{-5}$$

Then

$$x = 4.265$$

Therefore

$$4.265 = \frac{\mu}{2\sigma_x}$$

Or

$$\mu = (4.265)(2)(5.564 \times 10^{-15})$$

$$\mu = 6.36 \times 10^{-7} \text{ Amps}$$

To determine the proper threshold level, we would use the value calculated for μ , and then substitute it into Eq. (31).

Thus

$$\begin{aligned} k &= \frac{(6.36 \times 10^{-7})}{2} \\ &= 3.18 \times 10^{-7} \text{ Amps} \end{aligned}$$

Therefore, the threshold level must be set at 3.18×10^{-7} Amps. By changing the average current value, μ , in eq. (32), and using Eqs. (19), (20), (21), (22), and (23) the bit error rate can be determined for any altitude and path length. Using the fixed threshold value above, theoretical bit error rates for an increasing propagation path length, at any altitude, can be determined.

Summary

In modeling the effects of the turbulence, the Gujar Kavanaugh technique was used to produce a sequence of numbers which have a lognormal distribution and a low pass filter-like PSD. By taking the FFT of this turbulence sequence, it was found that its PSD actually resembled that of the intensity fluctuations. Once these sequence of numbers were generated, they were multiplied by the binary information signal. The result was a signal which faded with time. After undergoing the multiplicative effects of turbulence, the effects on the signal due the background radiation, were evaluated. It was found that the power associated with the background radiation was constant and a function of its spectral radiance. The receiver was assumed to be thermal noise limited and the shot noise due to the background radiation was assumed to be normally distributed. Thus, gaussian statistics could be used in determining the bit error rate and the optimum threshold level.

IV. Results of the Simulation

Introduction

This chapter examines the performance of the on/off keying air-to-air optical communication link. The performance results for this link have been presented in terms of the bit error rate plotted against the propagation path lengths.

In determining the performance of this communication system, a total of nine different links were chosen to be evaluated. The performance parameters associated with these links are listed in Table III. On the whole, these links were chosen such that they represented potential operating environments of the larger operational aircraft in the Air Force inventory. By varying the altitude, aircraft speed, and data rate a basic understanding of how these parameters can affect the performance of the link can be achieved.

The next logical step in the performance determination is to develop a baseline link. For the purpose of this thesis, the baseline link will be assumed to operate under the identical conditions of the simulated air-to-air link; except that it will not be influenced by the effects of turbulence. By comparing the air-to-air link with the baseline link, an understanding of how atmospheric turbulence affects these optical links can be achieved.

Table III

Parameters of the communication links used

Altitude (ft)	True Aircraft Speed (knots)	Data Rate (bps)
10,000	425	20,000
10,000	425	40,000
10,000	475	20,000
20,000	425	20,000
20,000	425	40,000
20,000	475	20,000
30,000	425	20,000
30,000	425	40,000
30,000	475	20,000

Table IV

Transmitter and Receiver Characteristics

Transmitter Output Power: 50 W
 Transmitter Optics Efficiency: 0.9
 Transmitter and Receiver Aperture Diameters: 0.127 m
 Receiver Optics Efficiency: 0.8
 Receiver Field of View: 3.848×10^{-5} sr
 Receiver Gain: 40

The equipment parameters used in this simulation are listed in Table IV. If desired, the choice of these parameters could be purely arbitrary. Changing any of the parameter values doesn't cause any problems with the simulation software.

Originally, the software for this simulation was written on AFIT's VAX computer. However, the sheer number of calculations and IMSL subroutine calls proved to be much more than the VAX could efficiently handle. As a result, Aeronautical Systems Division's (ASD) CYBER computer system had to be used. This system proved to be more capable of running the simulation.

Performance of the Baseline System

By using the bit error rate analysis described in Chapter III, baseline link performance curves were generated. Although these curves do not include the effects of turbulence; thermal current and shot noise due to the background radiation are accounted for.

The baseline link performance curves are plotted in Figures 16, 17, and 18. As shown, the bit error rate rises, from 5×10^{-5} to .5, as the propagation path length increases. This "fluid" bit error rate is due to the fact that as the path length increases, the received signal strength decreases. As a result, the thermal current and the shot noise, due to the background radiation, begin to dominate over the signal.

Since our threshold levels have been designed for a minimum bit error rate of 10^{-5} , it can be said that the system has a certain "reliability range." This reliability range corresponds to the maximum range that the link can

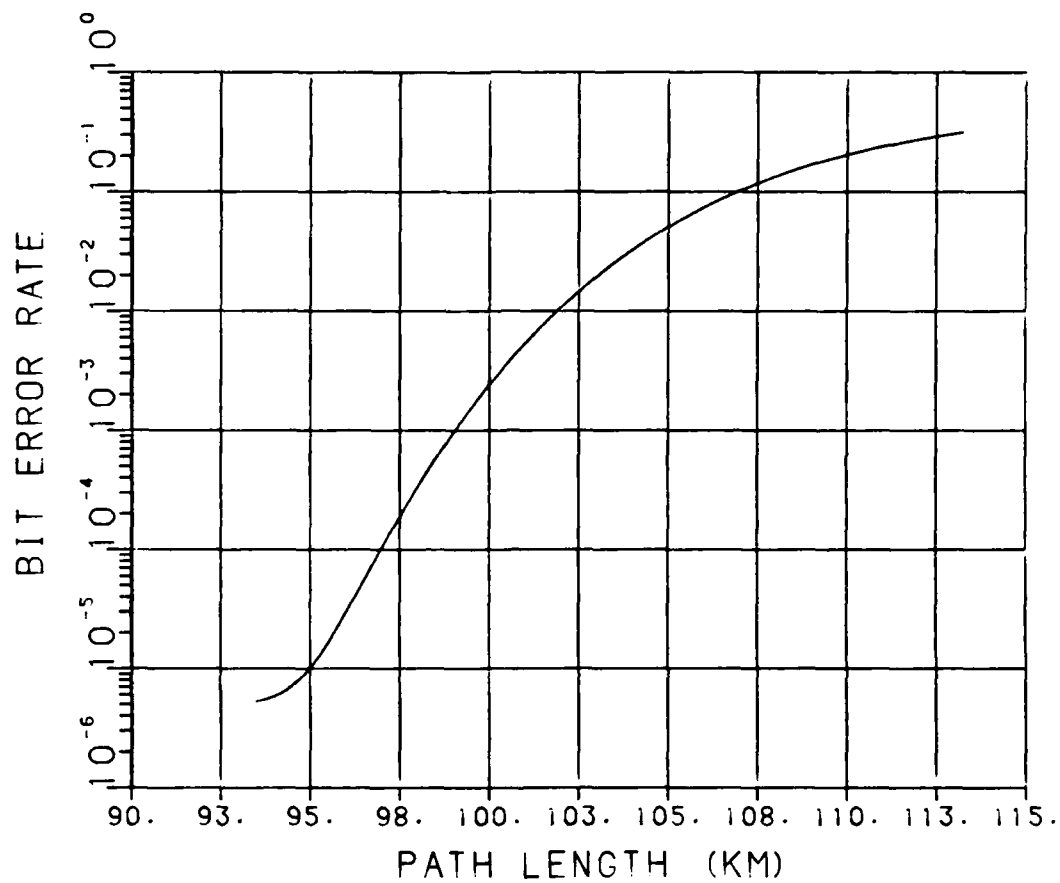


Figure 16. Theoretical bit error rate for an altitude of 10,000 ft.

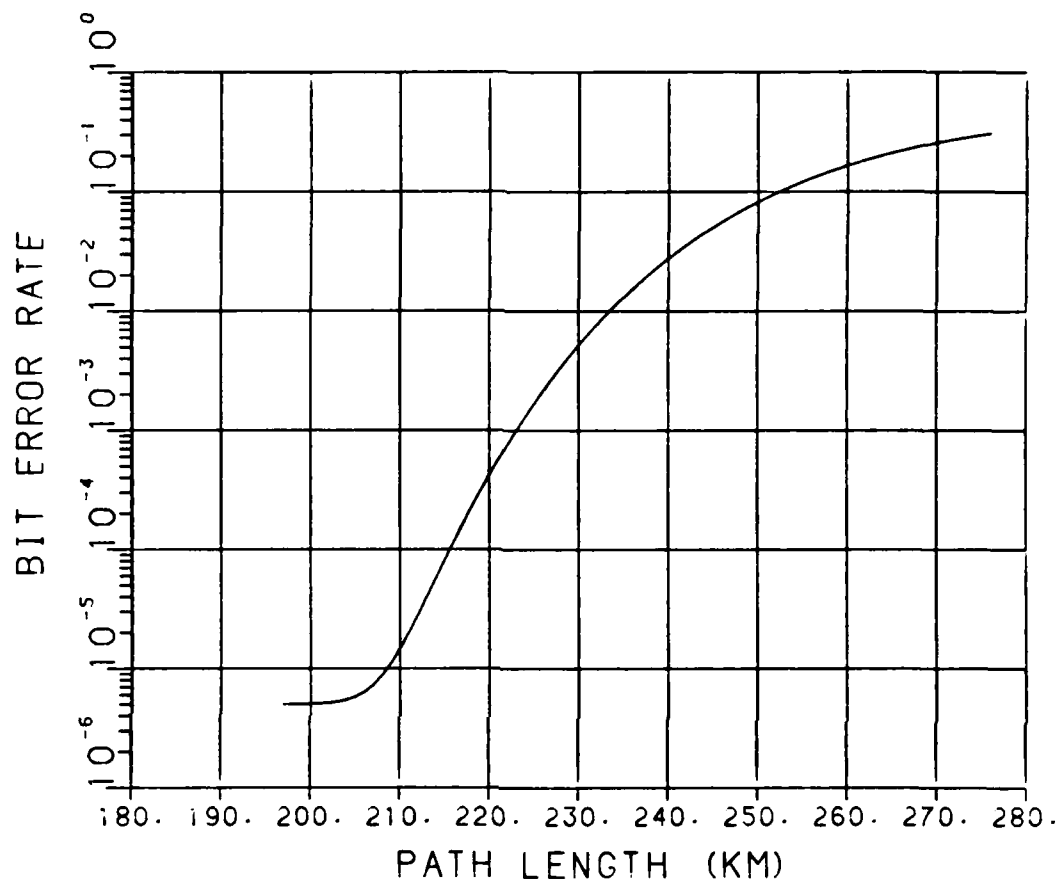


Figure 17. Theoretical bit error rate for an altitude of 20,000 ft.

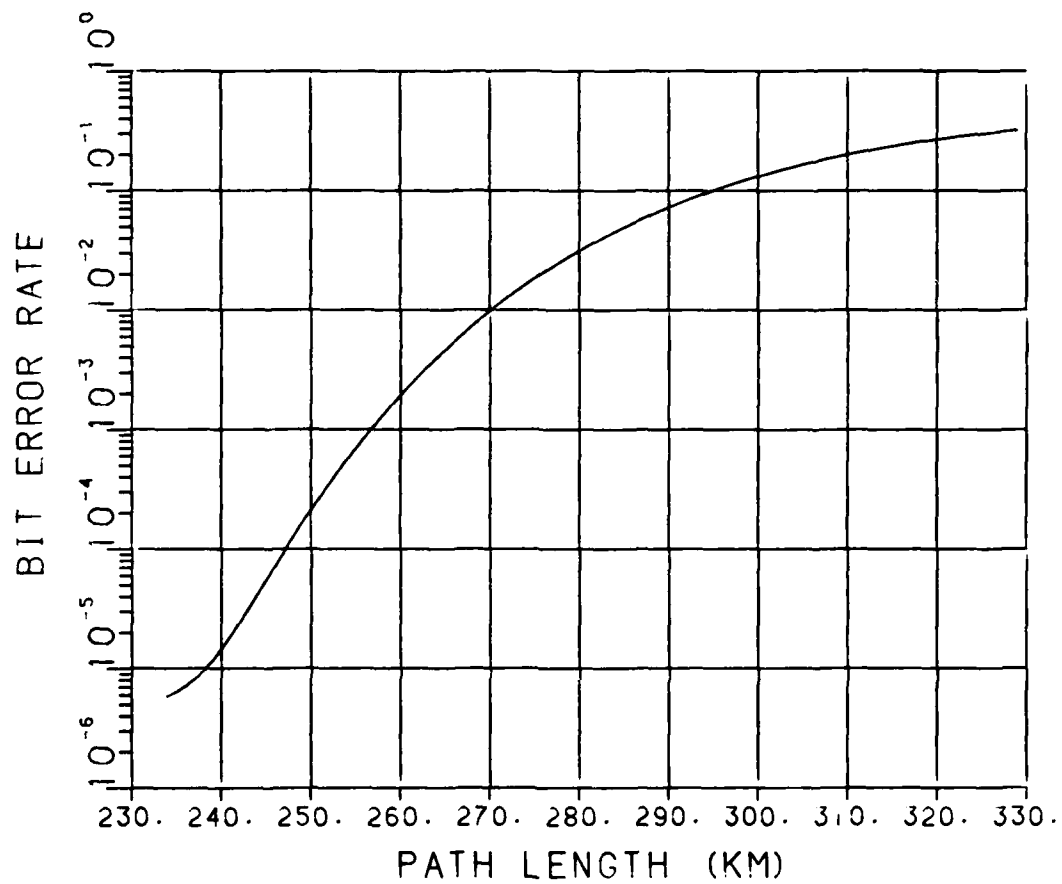


Figure 18. Theoretical bit error rate for an altitude of 30,000 ft.

operate while still maintaining a bit error rate of at least 10^{-5} . From Figures 16, 17, and 18, it can be seen that these maximum reliable ranges are 95 km, 208 km, and 239 km, respectively.

Although the received power of the signal is the dominant factor in determining the bit error rate, this power is a function of many factors. Factors such as: path length, field of view, and receiver optics play key roles in determining what the received power levels will be. However, the absorption and scattering coefficients are the factors that allow each link to obtain longer maximum reliable ranges with an increase in the altitude. These coefficients determine the amount of transmitted signal power which passes through the atmosphere, unattenuated, to the receiver. The higher the value of these coefficients, the larger the amount of received signal power. As the altitude is increased, these values typically increase.

By looking at these performance curves it becomes obvious that the maximum reliable range gets longer as the altitude is increased. This is primarily due to the fact that there is less of a concentration of aerosols (i.e. dust, smoke, smog, etc...) in the higher altitudes. Thus, there is less scattering of the optical beam.

Performance of the Actual Optical Link

The computer simulation was run, and the necessary performance data points were generated for the nine links shown in Table III. The results of these runs were broken up into three altitude groups; namely, 10000 ft, 20000 ft, and 30000 ft. In turn, each of these groups were broken down into three subgroups; where each subgroup consists of links with varying aircraft speeds and data rates.

The results of the computer simulation for the 10,000 ft altitude group can be seen in Figures 19, 20, and 21, and the results for the 20,000 ft links are shown in Figures 22, 23, and 24. Figures 25, 26, and 27 present those results for 30,000 ft. The data points used to generate these performance plots are listed in Appendix A.

By comparing Figures 19 - 27 with the baseline links shown in Figures 16, 17, and 18, the effects of turbulence can clearly be seen. As shown, atmospheric turbulence severely degrades the performance of the optical link. Table V compares the maximum reliable communication ranges of the turbulence induced link vs. those of the baseline link. As shown, the maximum reliable ranges are degraded anywhere from 50 to 66 percent; depending upon the link analyzed. This amount of degradation could have a severe impact on the operational environment of any optical communication system.

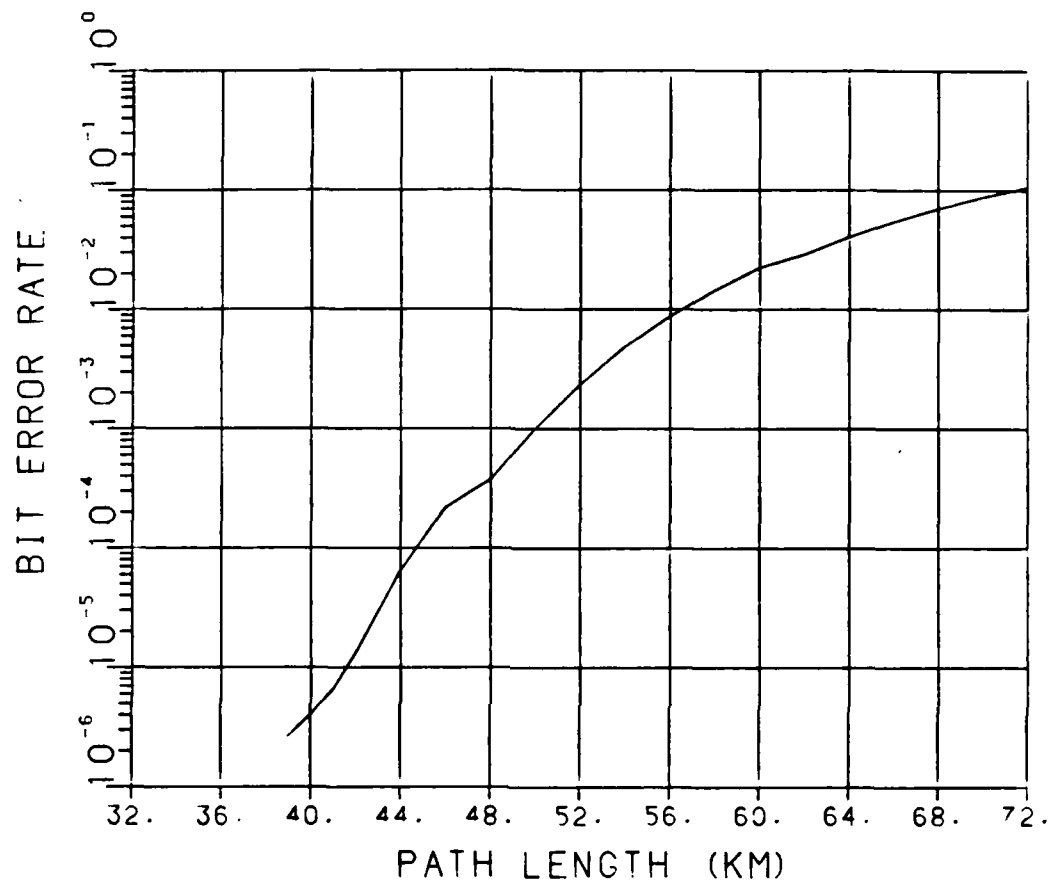


Figure 19. Turbulence affected optical link.
Altitude: 10,000 ft
Aircraft speed: 425 knts
Data rate: 20,000 bps

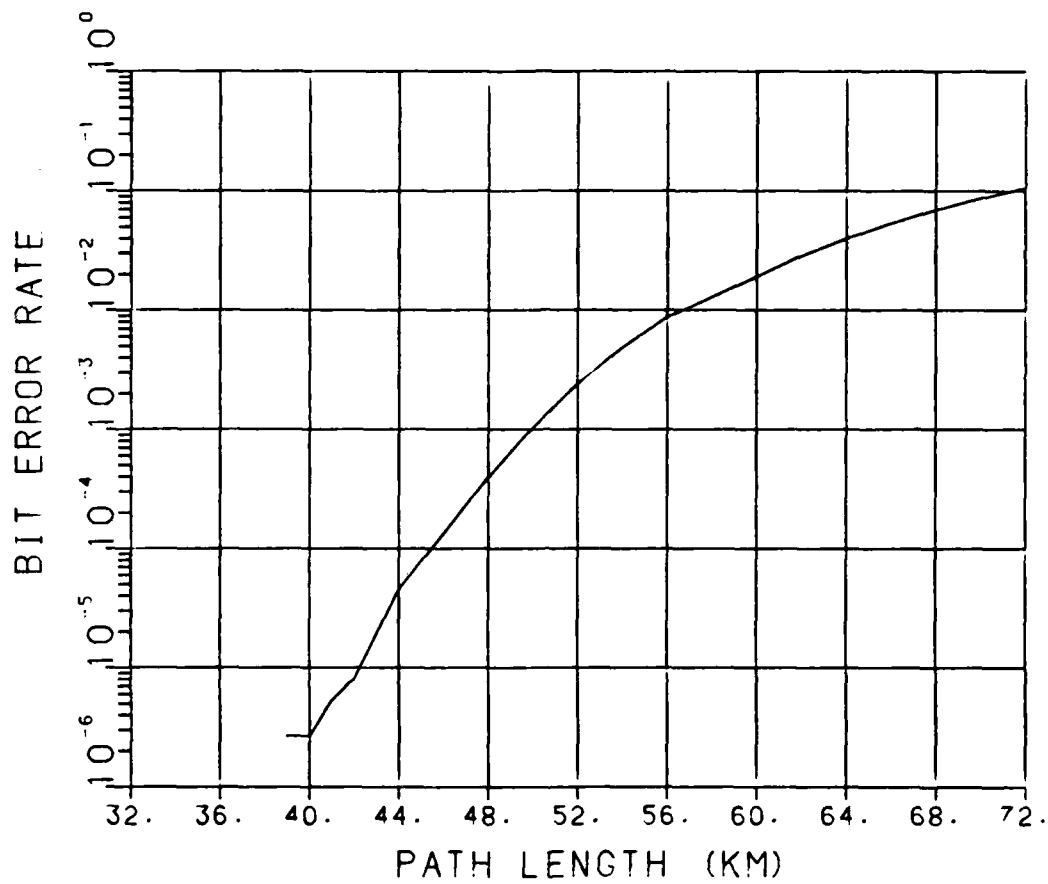


Figure 20. Turbulence affected optical link.
Altitude: 10,000 ft
Aircraft Speed: 475 knts
Data rate: 20,000 bps

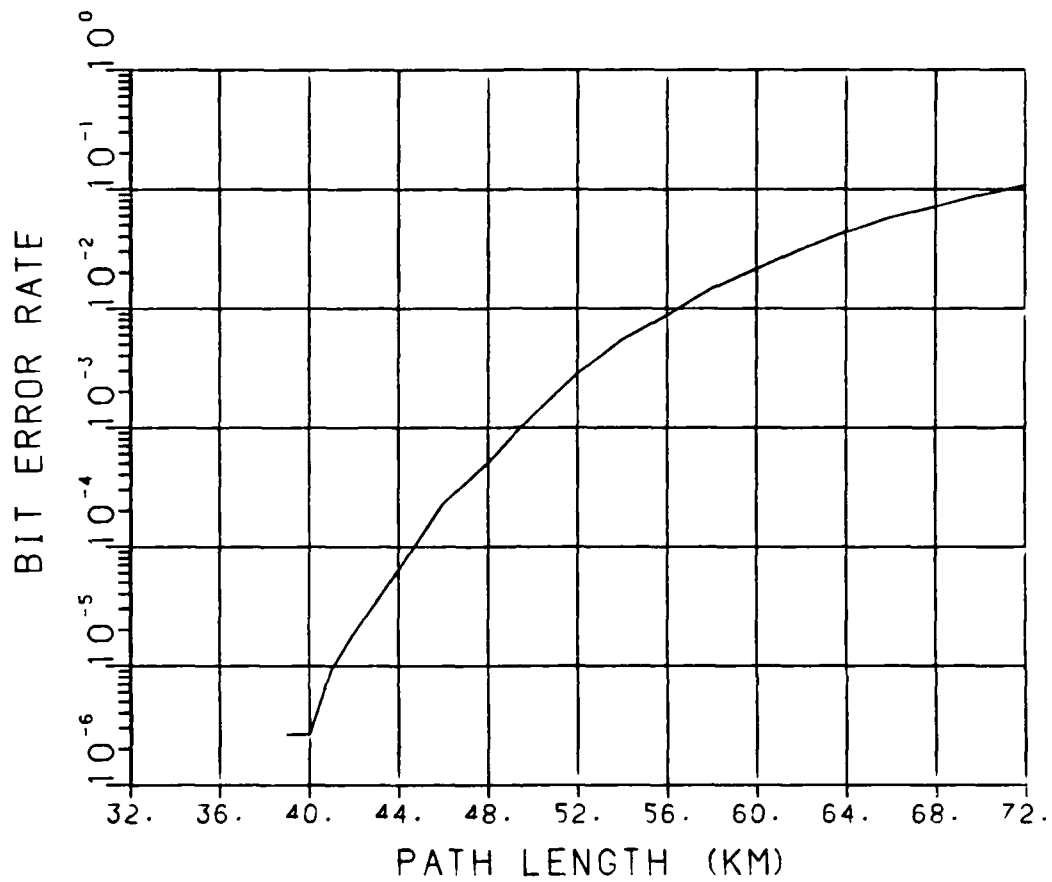


Figure 21. Turbulence affected optical link.
Altitude: 10,000 ft
Aircraft speed: 425 knts
Data rate: 40,000 bps

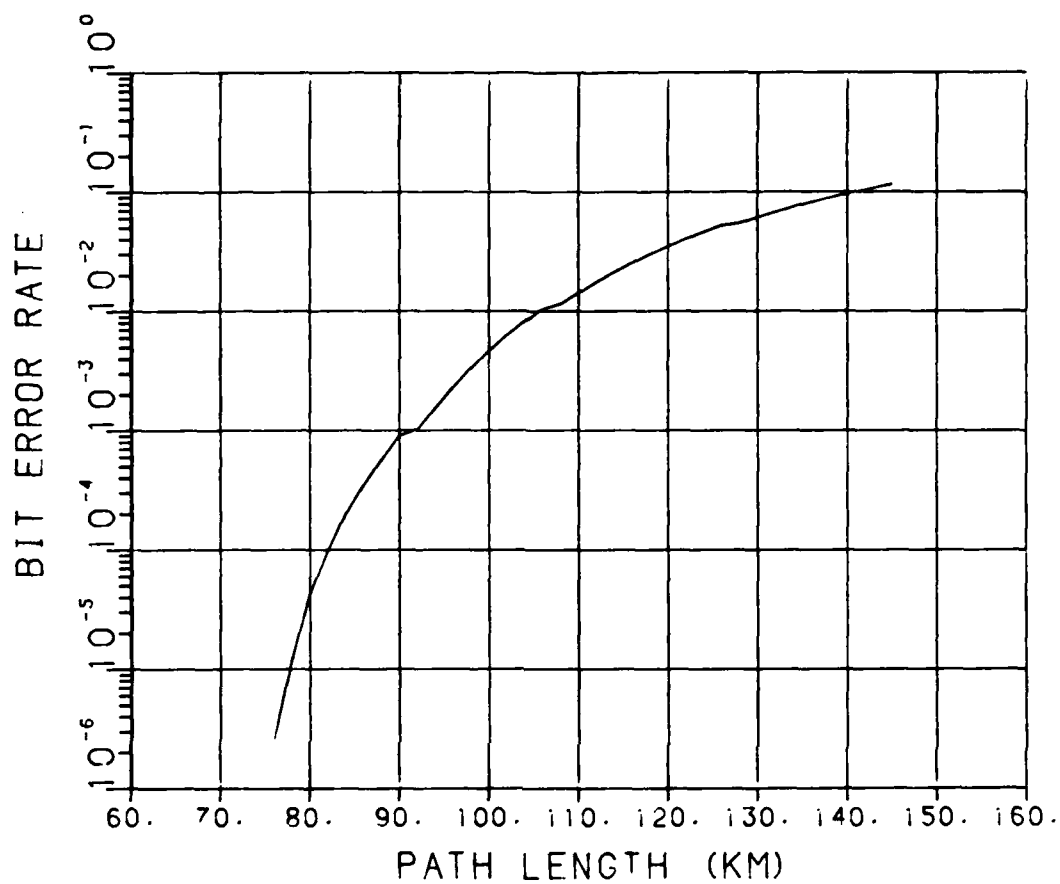


Figure 22. Turbulence affected optical link.
Altitude: 20,000 ft
Aircraft speed: 425 knts
Data rate: 20,000 bps

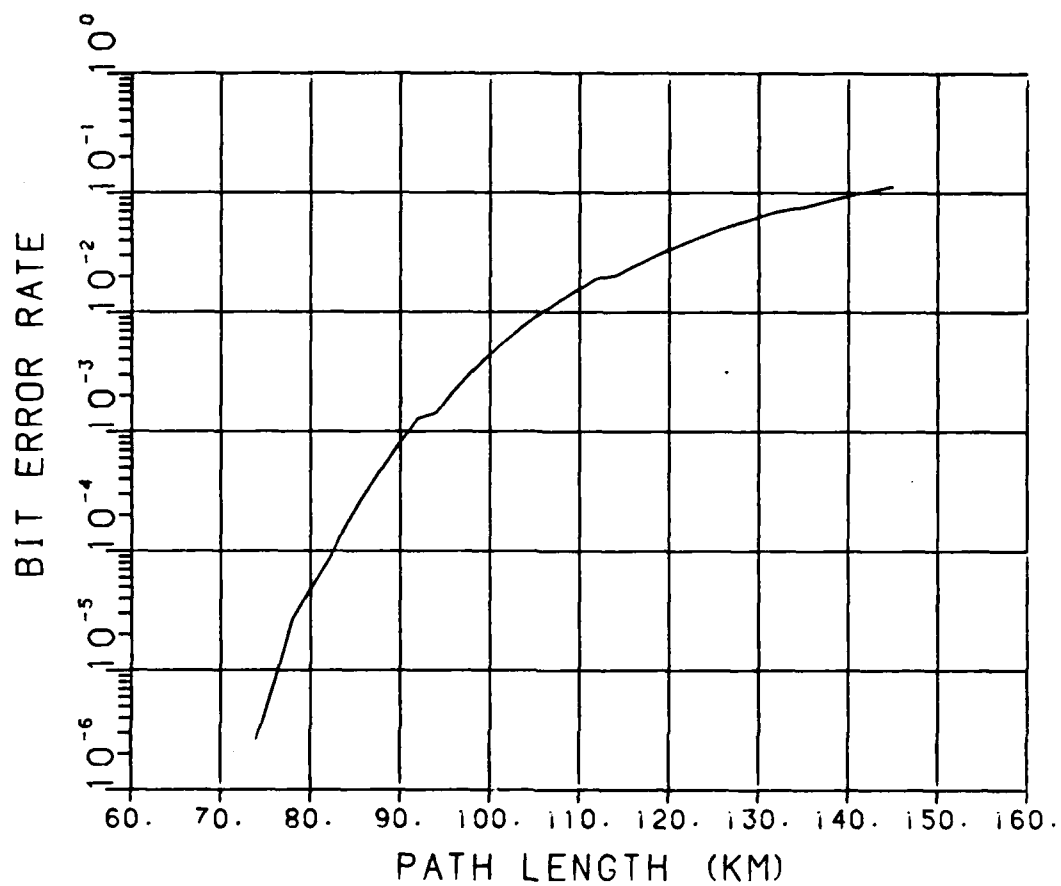


Figure 23. Turbulence affected optical link.
Altitude: 20,000 ft
Aircraft speed: 475 knts
Data rate: 20,000 bps

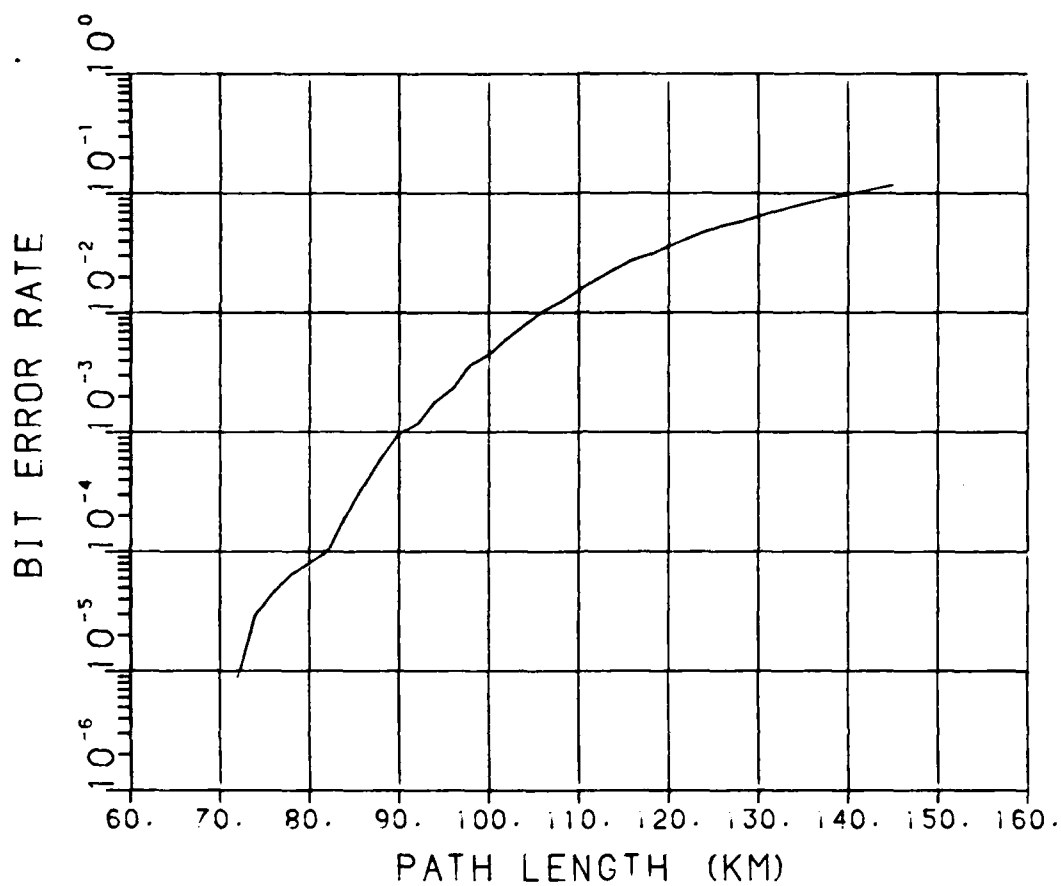


Figure 24. Turbulence affected optical link.
Altitude: 20,000 ft
Aircraft speed: 425 knts
Data rate: 40,000 bps

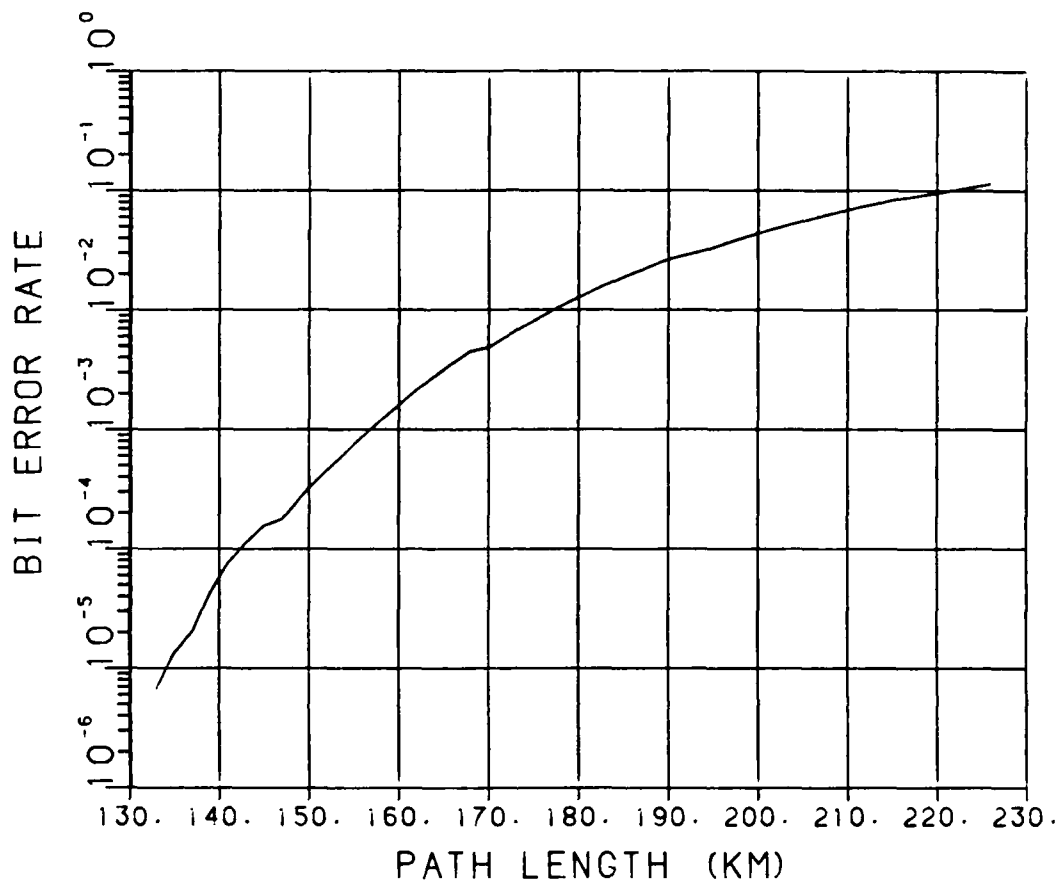


Figure 25. Turbulence affected optical links.
Altitude: 30,000 ft
Aircraft speed: 425 knts
Data rate: 20,000 bps

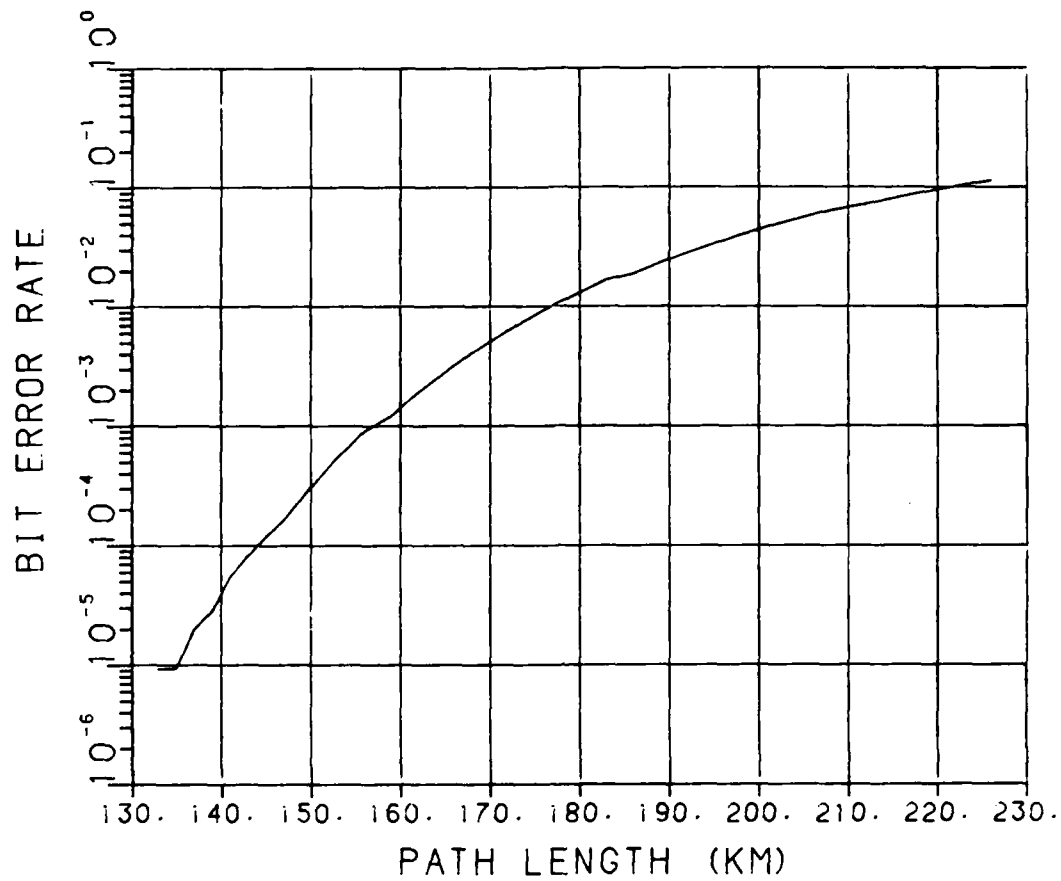


Figure 26. Turbulence affected optical link.
Altitude: 30,000 ft
Aircraft speed: 475 knts
Data rate: 20,000 bps

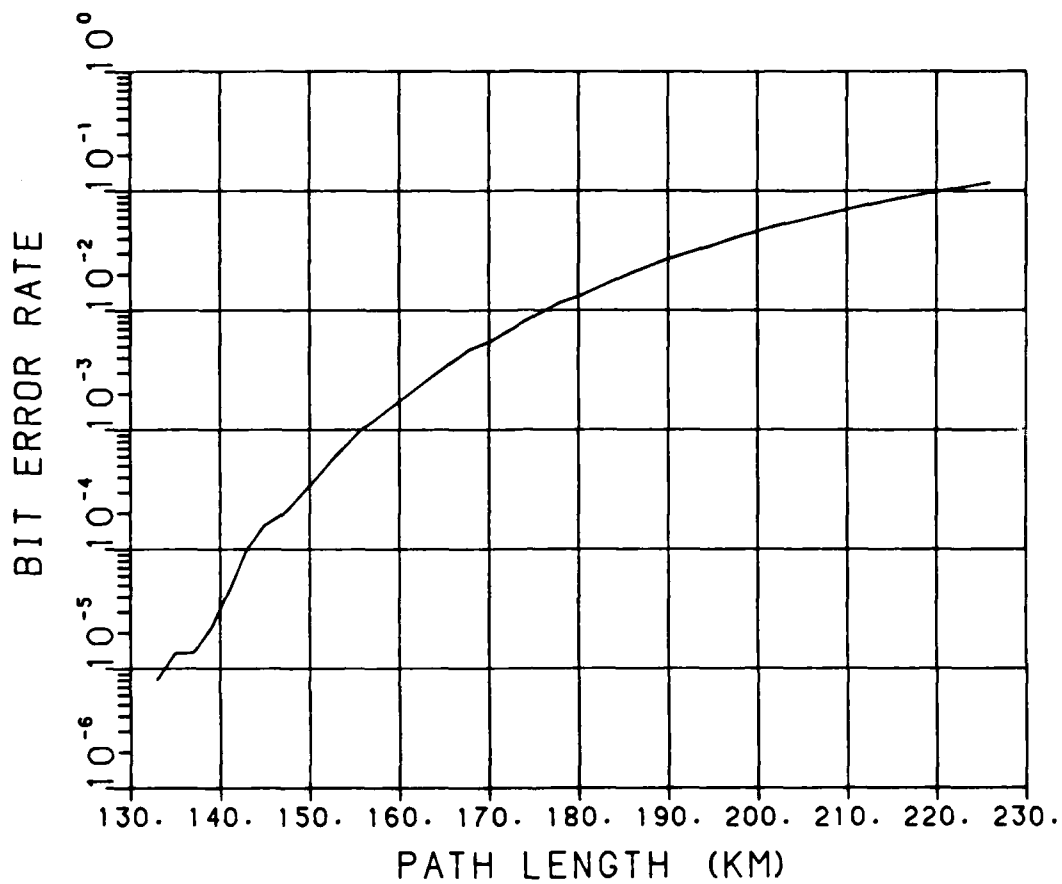


Figure 27. Turbulence affected optical link.
Altitude: 30,000 ft
Aircraft speed: 425 knts
Data rate: 40,000 bps

Table V

Maximum reliable ranges for the baseline link
and the turbulence affected links

Altitude (ft)	Reliable Ranges	
	Baseline Link (km)	Turbulence Link (km)
10,000	95	≈ 42
20,000	208	≈ 77
30,000	239	≈ 134

Further analysis of the performance curves, and the data in Appendix A, of each altitude group, yielded some interesting results. Namely, the plots of each altitude group show that as the aircraft speed is increased, from 425 knots to 475 knots, the bit error rates didn't appear to change significantly. This could be due to the fact that the change in velocity (50 knots) was relatively small.

However, the fact remains that the speed of the aircraft doesn't affect the strength of the turbulence. Instead, variations in speed will only effect the frequency content of the intensity fluctuation power spectral density (IFPSD). From Eq. (20) in Chapter II, it was shown that the highest frequency component, f_0 , present in the IFPSD can be expressed as

$$f_o = \frac{ws}{\sqrt{2\pi\lambda L}}$$

where

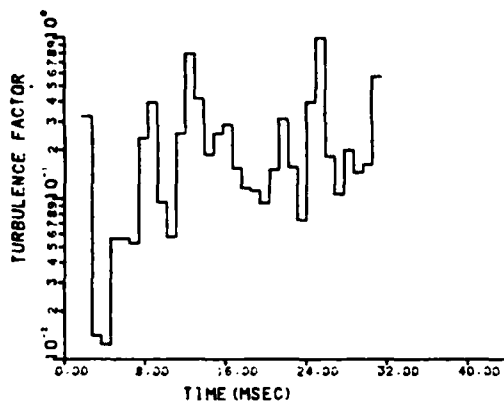
ws = aircraft speed

L = propagation path length

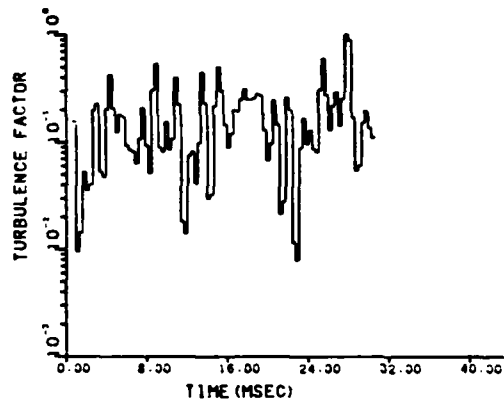
From this relation, it can be seen that for equivalent path lengths, the IFPSD contains higher frequency components for faster aircraft speeds. This means that the optical beam's intensity fluctuations will vary more rapidly as the speed of the aircraft is increased.

An example of this is shown in Figure 28. As shown, the first 32 msec of the 200 knot turbulence factor sequences have been compressed (and are equivalent) to the first 11 msec of the 600 knot sequences. This clearly shows that as the speed is increased, the turbulence factors vary more quickly. However, their maximum and minimum values are not affected by the aircraft's speed. From this figure, it can be determined that the variance of the log amplitude is responsible for inducing larger fluctuations of turbulence factor values.

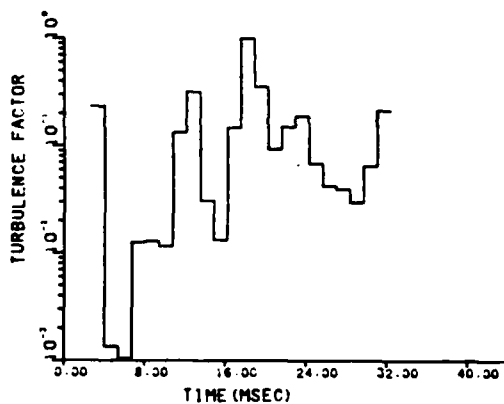
A sample turbulence factor sequence for 425 knots and 475 knots is shown in Figure 29. As shown, the sequence at 475 knots is slightly more compressed than the one at 425 knots. This close similarity in these sequences is the reason for similar bit error rates at different aircraft speeds. One could then reasonably assume that as the difference in aircraft speeds got larger the bit error rates



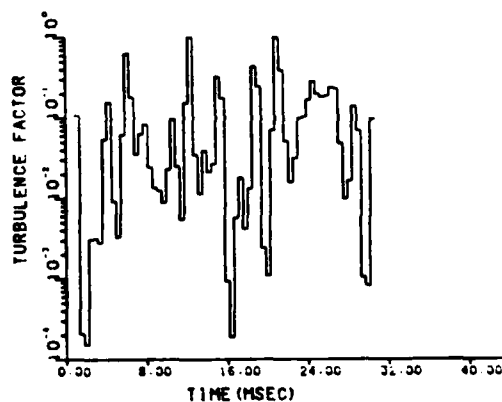
a. Aircraft Speed: 200 knots
Variance: .0976



b. Aircraft Speed: 600 knots
Variance: .0976

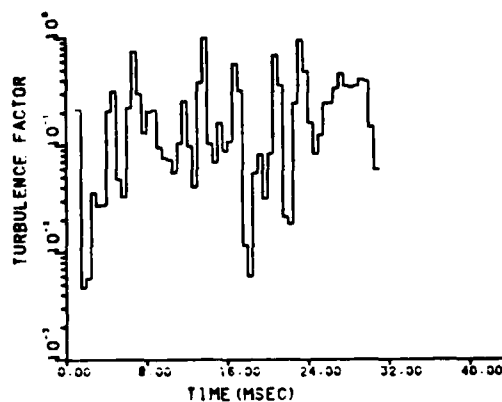


c. Aircraft Speed: 200 knots
Variance: .3947

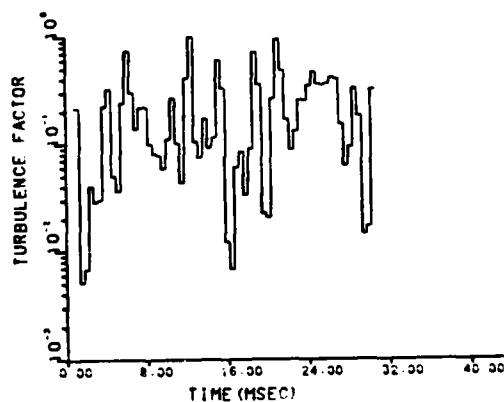


d. Aircraft Speed: 600 knots
Variance: .3947

Figure 28. Representation of possible turbulence factor sequences.



a. Aircraft Speed: 425 knots
Variance: .1469



b. Aircraft Speed: 475 knots
Variance: .1469

Figure 29. Representation of the turbulence factor sequences for an altitude of 20,000 ft and a 70 km path length.

could be expected to differ by a more significant amount. However, one must remember that the larger and more typical aircraft in the Air Force fleet tend to cruise at speeds

Thus, the variance of the log amplitude is the dominant factor in determining the values of the turbulence factors. From the data in Appendix A, it can also be shown that as the variance gets ranging from 375-500 knots; a difference of only 125 knots. Therefore, it can be concluded that increasing or decreasing the speed of the aircraft will not have a dramatic impact on the link bit error rates.

Thus, the variance of the log amplitude is the dominant factor in determining the values of the turbulence factors. From the data in Appendix A, it can also be determined that as the variance gets larger, the "strength" of the turbulence increases, and the bit error rate rises. From Chapter II it was shown that the variance could be expressed as:

$$\sigma_X^2 = .124 C_n^2 (k)^{7/6} (L)^{11/6}$$

where

k^2 = wavenumber
 C_n^2 = refractive index structure constant
 L = propagation path length

Since "k" is a constant throughout the entire simulation, the variance becomes a function of both C_n^2 and the path length. Values of C_n^2 for altitudes of 10000 ft, 20000 ft, and 30000 ft have been calculated to be 6.4×10^{-17} , 1.617×10^{-17} , and 1.947×10^{-18} , respectively. By comparing

the differences between C_n^2 for each of the altitudes analyzed, it is easy to see that they differ by multiples of an order of magnitude. Since the propagation path lengths, for the various links, differ from each other by no more than factors of 2 and 3, C_n^2 can be considered to be the dominant factor in determining the value of the variance. However, the value of C_n^2 is determined by the altitude of the aircraft. Therefore, it is the altitude which plays the key role in determining the range of reliable communications and the bit error rate. The higher the altitude, the longer the reliable range becomes.

However, one cannot keep increasing the altitude indefinitely. For example, Figure 4 (page 16), illustrates that thermal inversions within the tropopause which occur at approximately 35,000 ft cause the values of C_n^2 to increase. As a result, the variance increases and the maximum reliable ranges decrease. Therefore, for a given optical communication system, a prudent choice of altitudes could minimize the bit error rates, while at the same time maximizing the reliable communication ranges.

Increasing the data rate, proved to consistently raise the bit error rate in all of the links analyzed. Examining this situation further, it was found that increasing the data rate forced more bits to be multiplied by a singular turbulence factor. For example, if we had 1 turbulence factor for every 5 signal bits, then doubling the data rate

would yield 1 turbulence factor for every 10 signal bits. If there happened to be a prolonged fade, for example, 3 or 4 sequential turbulence factors having very small values, then there is a potential to "wipe-out" a string of 40 sequential signal bits.

Summary

In conclusion, the computer simulation was run, and the results were compared with those of the baseline link. Also, assessments were made as to how atmospheric turbulence affects the air-to-air optical link. The next chapter, Chapter V, summarizes the conclusions reached from this project, and presents recommendations for future work.

V. Conclusions and Recommendations

Conclusions

The goal of this project was to determine the performance of an air-to-air optical communication link, and to evaluate the effects of atmospheric turbulence. A major part of this task was the development of the computer simulation which determined the bit error rates from various optical links. Using this simulation, performance results were obtained for nine different turbulence influenced links. By comparing the data from these links with the baseline links, it was possible to evaluate the effects of turbulence. The results of both the baseline link and the computer simulation links have been presented in the form of performance curves. A summary of the conclusions reached are presented as follows

1. By comparing the baseline link with the turbulence influenced links it was found that atmospheric turbulence severely degraded the performance of the analyzed communication link. Losses of from 50 to 66 percent, over the theoretical maximum in reliable communication ranges were not uncommon.
2. Although the speed of the communicating aircraft was only increased by 50 knots, the differences in bit error rates (at comparable altitudes) was insignificant. This was

due to the fact that the aircraft's speed only affects the rapidness of the intensity fluctuations and not the strength. Larger differences in aircraft speed might produce more significant results.

3. The variance of the log amplitude was found to be the dominant factor in determining the strength of the turbulence. Larger values of the variance tended to increase the link bit error rate. It was shown that C_n^2 plays a key role in the determination of the value of the variance. Since C_n^2 is directly related to the altitude, a prudent choice of altitudes could provide longer reliable communication ranges.

4. Increasing the data rates of the links tended to increase the bit error rates. This was due to more signal bits being multiplied by fewer turbulence factors. If the data rate were slowed down, then (for the purposes of this simulation) there would be fewer signal bits being affected by a singular turbulence factor. Ideally, one would want the data rate at such a speed that multiple turbulence factors would affect a single signal bit. Then, using an integrate and dump type receiver, the signal bit could be recovered. Slowing the data rate, in this way, allows us to average the effects of the turbulence factors. However, there is a limit as to how slow a potential user would like his data rate to be.

5. It was also found that the saturation region was never reached until bit error rates of approximately .3 - .35 . This means that within reliable communication ranges lognormal statistics can always be used to evaluate the effects of turbulence for a communication link.

Recommendations

Several follow-on efforts have become evident as a result of the work performed during the period of this thesis. The following recommendations are submitted

1. The analysis of the communication link was based on an on/off keying system. Since these types of systems aren't in common use today, the simulation could be modified to include various other types of modulation schemes. Once these other schemes have been programmed, a performance comparison of one scheme verses another could be done. As a result of these comparisons, a recommendation could be made as to which modulation scheme provides the best performance.
2. The present simulation does not include any coding of the information signal. An investigation into the various coding and interleaving schemes could be performed. This might give some insight into which coding schemes might prove to be the most effective against turbulence.

3. This simulation also assumes a simple threshold detector as the decision making device. It might prove to be more realistic if a matched filter device were used instead. This could be done by modifying the computer simulation.

Appendix A

Data Points

Altitude: 10,000 feet

Aircraft Speed(knots):	425	475	425
Data Rate(Kbps):	20	20	40

Path Length (km)	Variance
---------------------	----------

38	.1898	2.667 E-6	2.667 E-6	2.667 E-6
39	.1990	2.667 E-6	2.667 E-6	2.667 E-6
40	.2085	4.000 E-6	2.667 E-6	2.667 E-6
41	.2181	6.667 E-6	5.347 E-6	9.333 E-6
42	.2280	1.333 E-5	8.020 E-5	1.867 E-5
44	.2483	6.533 E-5	4.545 E-5	6.400 E-5
46	.2694	2.200 E-4	1.333 E-4	2.320 E-4
48	.2912	3.769 E-4	3.960 E-4	5.109 E-4
50	.3139	1.013 E-3	1.037 E-3	1.277 E-3
52	.3373	2.362 E-3	2.408 E-3	2.854 E-3
54	.3614	4.892 E-3	4.900 E-3	5.519 E-3
56	.3863	8.811 E-3	8.712 E-3	8.803 E-3
58	.4120	1.458 E-2	1.458 E-2	1.480 E-2
60	.4384	2.240 E-2	1.914 E-2	NC
62	.4656	2.891 E-2	2.856 E-2	3.158 E-2
64	.4935	4.060 E-2	4.002 E-2	4.409 E-2
66	.5221	5.462 E-2	5.374 E-2	5.856 E-2
68	.5515	7.065 E-2	6.957 E-2	7.205 E-2
70	.5816	8.785 E-2	8.704 E-2	8.951 E-2
72	.6124	0.107	0.106	0.108

NC denotes "not calculated"

AD-A151 840

THE EFFECTS OF ATMOSPHERIC TURBULENCE ON AN AIR-TO-AIR
OPTICAL COMMUNICATION LINK(U) AIR FORCE INST OF TECH
WRIGHT-PATTERSON AFB OH SCHOOL OF ENGI.. J N KANAVOS
DEC 84 AFIT/GE/ENG/84D-38 F/G 17/2

2/2

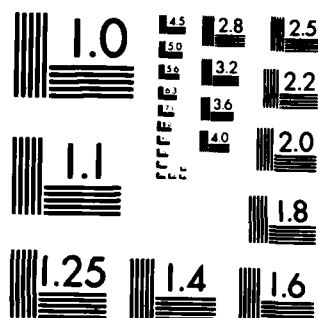
UNCLASSIFIED

NL

END

FORM D

DTM



MICROCOPY RESOLUTION TEST CHART
NATIONAL BUREAU OF STANDARDS-1963-A

Data Points

Altitude: 20,000 feet

Aircraft Speed(knots):	425	475	425
Data Rate(Kbps):	20	20	40

Path Length (km)	Variance
---------------------	----------

76	.1709	2.667 E-6	8.000 E-6	4.546 E-5
78	.1792	1.201 E-5	2.667 E-5	6.416 E-5
80	.1879	4.270 E-5	4.800 E-5	NC
82	.1964	9.874 E-5	8.266 E-5	9.875 E-5
84	.2053	2.002 E-4	1.680 E-4	1.939 E-4
86	.2143	3.496 E-4	2.973 E-4	3.515 E-4
88	.2235	5.725 E-4	4.973 E-4	6.034 E-4
90	.2329	9.061 E-4	8.173 E-4	9.616 E-4
92	.2425	1.024 E-3	1.292 E-3	1.168 E-3
94	.2523	1.552 E-3	1.435 E-3	1.786 E-3
96	.2622	2.317 E-3	2.199 E-3	2.317 E-3
98	.2723	3.329 E-3	3.192 E-3	3.690 E-3
100	.2826	4.676 E-3	4.429 E-3	4.485 E-3
102	.2930	6.321 E-3	6.005 E-3	6.064 E-3
104	.3036	8.201 E-3	7.950 E-3	NC
106	.3144	1.047 E-2	1.018 E-2	1.027 E-2
108	.3254	1.157 E-2	1.276 E-2	1.239 E-2
110	.3365	1.434 E-2	1.574 E-2	1.536 E-2
112	.3478	1.765 E-2	1.920 E-2	1.904 E-2
114	.3593	2.139 E-2	2.032 E-2	2.302 E-2
116	.3710	2.548 E-2	2.429 E-2	2.759 E-2
118	.3828	3.002 E-2	NC	3.072 E-2
120	.3947	3.499 E-2	3.347 E-2	3.590 E-2
122	.4069	4.039 E-2	3.868 E-2	4.159 E-2
124	.4192	4.620 E-2	4.421 E-2	4.749 E-2
126	.4317	5.240 E-2	5.032 E-2	5.354 E-2
128	.4443	5.480 E-2	5.662 E-2	5.775 E-2
132	.4701	6.801 E-2	7.006 E-2	7.111 E-2
135	.4899	7.857 E-2	7.667 E-2	8.145 E-2
140	.5237	9.672 E-2	9.529 E-2	9.816 E-2
145	.5585	0.116	0.115	0.117

Data Points

Altitude: 30,000 feet

Aircraft Speed(knots):
Data Rate(Kbps):

425
20

475
20

425
40

Path Length Variance
(km)

133	.0539	6.723 E-6	9.330 E-6	8.081 E-6
135	.0589	1.344 E-5	9.364 E-6	1.347 E-5
137	.0606	2.017 E-5	2.007 E-5	1.361 E-5
139	.0622	4.303 E-5	2.809 E-5	2.177 E-5
141	.0639	7.664 E-5	5.485 E-5	4.490 E-5
143	.0656	1.129 E-4	8.161 E-5	9.932 E-5
145	.0672	1.560 E-4	1.191 E-4	1.592 E-4
147	.0690	1.773 E-4	1.632 E-4	1.965 E-4
150	.0716	3.253 E-4	3.077 E-4	3.418 E-4
153	.0742	5.360 E-4	5.472 E-4	6.149 E-4
156	.0769	8.800 E-4	9.110 E-4	1.040 E-3
159	.0796	1.388 E-3	1.219 E-3	NC
162	.0824	2.153 E-3	1.939 E-3	NC
164	.0843	2.789 E-3	2.498 E-3	2.904 E-3
166	.0862	3.592 E-3	3.222 E-3	3.748 E-3
168	.0881	4.509 E-3	4.104 E-3	4.743 E-3
170	.0900	4.861 E-3	5.113 E-3	5.433 E-3
172	.0920	5.976 E-3	6.317 E-3	6.625 E-3
174	.0939	7.329 E-3	7.715 E-3	8.118 E-3
176	.0959	8.947 E-3	9.341 E-3	9.753 E-3
178	.0979	1.077 E-2	1.105 E-2	1.168 E-2
180	.1000	1.270 E-2	1.309 E-2	1.309 E-2
183	.1030	1.624 E-2	1.672 E-2	NC
186	.1061	2.020 E-2	1.889 E-2	2.070 E-2
190	.1104	2.656 E-2	2.480 E-2	2.704 E-2
194	.1147	3.142 E-2	3.169 E-2	3.344 E-2
198	.1190	3.950 E-2	3.983 E-2	4.178 E-2
202	.1235	4.857 E-2	4.904 E-2	5.098 E-2
208	.1303	6.380 E-2	6.384 E-2	6.483 E-2
212	.1349	7.471 E-2	7.222 E-2	7.595 E-2
216	.1396	8.622 E-2	8.375 E-2	8.745 E-2
220	.1444	9.552 E-2	9.574 E-2	9.839 E-2
226	.1517	0.114	0.114	0.117

Appendix B

FORTRAN Program Computer Code Listing

```
PROGRAM SINT
*****
* PROGRAM SINT   WRITTEN BY: JAY N. KANAVOS, CAPT, USAF *
* THIS PROGRAM WILL COMPUTE THE BIT ERROR RATE FOR AN   *
* OPTICAL AIR-TO-AIR LINK GIVEN THE AIRSPEED, ALTITUDE, *
* PROPAGATION PATH LENGTH, AND DATA RATE.             *
*****
C234567890
      DOUBLE PRECISION SEED(2500)
      DIMENSION D1(2),Z(21),X(21),F(20),R(20),Y(21),SUM(834)
      REAL LAMDA
      COMMON FILCOA,FILCOB,FILCOC,FILCOD,ZETA,VAR,LAMDA,THERMN
      +,SHOTNO,GOLD1,RXPOW,POWSIG,THRES,RLOAD
      PRINT *, 'INPUT AIRCRAFT SPEED(KNTS),ALT(FT),PATH LENGTH(KM)'
      READ *,V,P,A
      VN=V*.51398
      PATH=P*1000.
      ALT=A*.30473
      N=625
      COUNT=0.
* THIS ROUTINE CALCULATES THE SEED NUMBERS FOR THE IMSL
* SUBROUTINES.
      DO 10 J=1,2500
      CALL GGURS(12345678.D0,2,D1)
      SEED(J)=IDINT(D1(1)*D1(2)*1.D8)
10    CONTINUE
* THE FOLLOWING REPRESENTS THE EQUIPMENT PARAMETERS
      EFF=.85
      LAMDA=9040.E-10
      CONST=6.62E-34*(3.E8/LAMDA)
      RLOAD=30.
      Q=1.6E-19
      BAND=5.E6
      POWN=5.85E-7
      GAIN=40.
* THERMN = THERMAL NOISE POWER
* SHOTNO = BACKGROUND RADIATION SHOT NOISE VARIANCE(POWER)
* THRES = THRESHOLD LEVEL OF RECEIVER
      THERMN=2.*BAND*2.*1.38E-23*300./RLOAD
      SHOTNO=2.*BAND*EFF*POWN*Q**2*GAIN**(2+.3)/CONST
      THRES=.5*4.264890793924*2.*SQRT(SHOTNO+THERMN)
      PI=3.1415926
* BR = BIT RATE
      BR=20000.
      X(1)=-.5
      RXAREA=(PI/4.)*.127**2
* BETA = AEROSOL SCALING FACTORS
      IF(ALT.LE.4000.)BETA=.2-.19*(ALT/4000.)
```

```

      IF(ALT.GT.4000. .AND. ALT.LE.7000.) BETA=.01-.004*((ALT
      +-4000.)/3000.)
      IF(ALT.GT.7000.) BETA=6.E-3-5.6E-3*((ALT-7000.)/9000.)
      ++.5*((ALT-7000.)/9000.)*(((ALT-7000.)/9000.)-1.)*1.12E-2
*   ATRAN = TRANSMISSIVITY OF ATMOSPHERE
*   FOV   = FIELD OF VIEW (SR)
*   RXPOW = RECEIVED SIGNAL POWER
*   POWSIG = AMOUNT OF SIGNAL CURRENT IN RECEIVER
      ATRAN=EXP(-.42*BETA*P)*EFF*.67
      FOV=(PI/4.)*7.E-3**2
      RXPOW=ATLAN*50.*RXAREA/(FOV*PATH**2)
      POWSIG=(EFF*RXPOW*Q*GAIN/CONST)**2
*   THIS SECTION WILL CONVERT THE NORMALIZED POWER SPECTRUM
*   INTO A DENORMALIZED POWER SPECTRUM
      DO 13 J=2,20
      X(J)=X(J-1)+.0625
13   CONTINUE
      B(1)=.4320
      B(2)=.4333
      B(3)=.4433
      B(4)=.4467
      B(5)=.45
      B(6)=.448
      B(7)=.4467
      B(8)=.44
      B(9)=.432
      B(10)=.4133
      B(11)=.3833
      B(12)=.3333
      B(13)=.2667
      B(14)=.1833
      B(15)=.0733
      B(16)=.065
      B(17)=.0407
      B(18)=.03
      B(19)=.02
      B(20)=.015
*****
*   THE VALUES FOR EACH POINT ON THE PSD PLOT ARE
*   DETERMINED HERE.
*           VN = WIND SPEED
*           L  = PATH LENGTH
*           FM = MAXIMUM FREQUENCY
*           FO = A NORMALIZATION FREQUENCY
*****
*   CN2 = REFRACTIVE INDEX STRUCTURE CONSTANT
*   VAR = VARIANCE OF THE LOG AMPLITUDE
      IF(ALT.LT.1000.) CN2=((5.3E-8-5.07E-8*((ALT-10.)/990.))
      +*4.6416)**2

```



```

      IF(ALT.GE.1000. .AND. ALT.LT.8000.) CN2=((2.3E-9+
+((ALT-1000.)/7000.)*(-1.97E-9))*4.6416)**2
      IF(ALT.GE.8000. .AND. ALT.LT.10000.) CN2=((3.3E-10+((ALT-
+8000.)/1000.)*(-3.E-11)+((ALT-8000.)/1000.)*(((ALT-8000.)
+/1000.)-1.)*.5*6.E-11)*4.6416)**2
      IF(ALT.GE.10000. .AND. ALT.LE.14000.) CN2=((3.3E-10+((ALT-
+10000.)/2000.)*3.17E-9+((ALT-10000.)/2000.)*(((ALT-10000.)
+/2000.)-1.)*.5*(-6.34E-9))*4.6416)**2
      VAR=.124*CN2*(2.*PI/LAMDA)**(7./6.)*(PATH)**(11./6.)
      FM=.32*VN/(LAMDA*PATH)**(.5)
      FO=VN/SQRT(PATH*LAMDA*2.*PI)
*****
*      F( ) = FREQUENCY VALUE
*      Y( ) = CORRESPONDING PSD VALUE
*      Y(21)= THE LAST POINT WITHIN THE .2 DB OF THE
*              MAXIMUM VALUE OF THE PSD
*****
      DO 11 J=1,20
      F(J)=FO*EXP(X(J))
      Y(J)=SQRT(B(J)*VAR/FO)
11    CONTINUE
      IF (FM.LT.F(5)) PRINT *, 'SORRY SOMETHING IS WRONG'
      DELTA1=F(6)-F(5)
      DELTA2=FM-F(5)
      DELTA3=DELTA2/DELTA1
      DIF1=Y(5)-Y(6)
      DIF2=DIF1*DELTA3
      Y(21)=DIF2+Y(5)
      DO 12 J=1,20
      Z(J)=Y(J)/Y(21)
12    CONTINUE
*****
*      THE 3 DB POINT IS CALCULATED HERE
*****
      DB=Y(21)/2.
      DO 33 J=1,20
      IF (DB.GE.Y(J)) GO TO 99
      GO TO 33
99    A=Y(J)
      BZ=Y(J-1)
      C=F(J)
      D=F(J-1)
      GO TO 98
33    CONTINUE
98    A1=BZ-A
      A2=BZ-DB
      BZ1=C-D
      BZ2=A2*BZ1/A1
      S=D+BZ2

```

```

SAMP=1./(3.*F(20))
*****
* THIS ROUTINE CALCULATES THE NEW SAMPLING TIME. *
* WE NEED A NEW SAMPLING TIME BECAUSE THE SCINTILLATION*
* MULTIPLICATIVE NUMBERS MUST BE USED AN INTERGER *
* MULTIPLE NUMBER OF TIMES. *
* BR = BIT RATE (20000 B/S) *
*****
GOLD=BR*SAMP
GOLD1=AIN(T(GOLD))
IF(GOLD1.GE.1.) GOLD1=GOLD1+1.
IF(GOLD1.LT.1.) GOLD1=1.
T=GOLD1/BR
*****
* RANDOM NUMBERS ARE GENERATED AND CHANGED INTO *
* NORMAL DISTRIBUTED NUMBERS. THESE NUMBERS ARE *
* THEN FED INTO THE FILTER, AND OUTPUTED. THE *
* OUTPUTED NUMBERS HAVE THE DESIRED PSD. *
*****
* THE FILTER COEFFICIENTS ARE DETERMINED HERE *
*****
951 S=(2./T)*TAN(T*S*PI)
COEF1=.81463413
COEF2=1.41362877
COEF3=COEF1
ALPHA=COEF1+COEF3
BETA=COEF1*COEF3+COEF2
DELTA=COEF2*COEF3
FILCOA=S**3*(T/2.):**3
FILCOB=ALPHA*S*(T/2.)
FILCOC=BETA*(S**2)*(T/2.):**2
FILCOD=DELTA*(S**3)*((T/2.):**3)
ZETA=1./(1.+FILCOB+FILCOC+FILCOD)
COUNT1=0.
* SUBROUTINE 'ERROR' ACTUALLY DETERMINES THE VALUES OF
* OF THE TURBULENCE FACTORS
DO 1 J=1,N
CALL ERROR(ALT,J,SEED(J),SEED(J+625),SEED(J+1250),
+SEED(J+1875),SUM(J),NR)
COUNT1=COUNT1+NR
COUNT=COUNT+SUM(J)
1 CONTINUE
PERROR=COUNT/COUNT1
SHANON=ALT/.30473
WRITE(*,4)PERROR,PATH,COUNT,SHANON,V
4 FORMAT( E15.8,3X,F10.2,2X,F10.2,3X,F10.1,2X,F5.1)
END
* IN ORDER TO ALLOW FOR EFFICIENT USE OF COMPUTER TIME,

```

```

* ONLY 1200 TURBULENCE FACTORS CAN BE DETERMINED AT
* ONCE.  THUS, SUBROUTINE 'ERROR' IS CALLED ABOUT
* 750,000/1200 = 625 TIMES
  SUBROUTINE ERROR(ALT,INDIA,DSEED,DSEED1,DSEED2,
+DSEED3,SUM,NR)
    DOUBLE PRECISION DSEED,DSEED1,DSEED2,DSEED3
    DIMENSION X1(-2:1200),Y1(-2:1200),R1(1200),
+R2(1200),SIGCUR(1200),TOTAL(1200),BACK(1200)
    REAL LAMDA,LNORM(1200),NOIS(1200)
    COMMON FILCOA,FILCOB,FILCOC,FILCOD,ZETA,VAR,LAMDA,THERMN
+ ,SHOTNO,GOLD1,RXPOW,POWSIG,THRES,RLOAD
    NR=1200
    K=INT(NR/INT(GOLD1))
    NR=IFIX(GOLD1)*K
    X1(0)=0.
    X1(-1)=0.
    X1(-2)=0.
    Y1(0)=0.
    Y1(-1)=0.
    Y1(-2)=0.
* R1 = INFORMATION SIGNAL (BINARY 1'S AND 0'S)
* X1 = GAUSSIAN DISTRIBUTED NUMBERS WHICH ARE FED
* INTO THE LINEAR FILTER
* NOIS = GAUSSIAN DISTRIBUTED THERMAL NOISE CURRENT VALUES
* BACK = GAUSSIAN DISTRIBUTED BACKGROUND SHOT NOISE
* CURRENT VALUES
* THE IMSL ROUTINES ARE CALLED HERE TO GENERATE THESE VALUES
    CALL GGU8S(DSEED1,NR,R1)
    CALL GGNML(DSEED,NR,X1)
    CALL GGNML(DSEED2,NR,NOIS)
    CALL GGNML(DSEED3,NR,BACK)
* THE OUTPUT SEQUENCE ( Y1(J) ) FROM THE LINEAR FILTER IS
* DETERMINED HERE, AS WELL AS THE VARIANCE OF THIS
* SEQUENCE ( AVEVAR )
    AVEVAR=0.
    DO 13 J=1,K
        Y1(J)=ZETA*(FILCOA*X1(J)+3.*FILCOA*X1(J-1)+
+3.*FILCOA*X1(J-2)+FILCOA*X1(J-3)-(FILCOC+
+3.*FILCOD-3.-FILCOB)*Y1(J-1)-(3.-FILCOB-
+FILCOC+3.*FILCOD)*Y1(J-2)-(FILCOB+FILCOD-
+1.-FILCOC)*Y1(J-3))
        AVEVAR=AVEVAR+(Y1(J)**2)
13    CONTINUE
    AVEVAR=AVEVAR/LOAT(K)
    DELTAZ=.0001
    VAR1=SQRT(VAR)
    IF(INDIA.GT.1)GO TO 1
    CALL DELTA(VAR,DELTAY)

```

```

* THE GAUSSIAN DISTRIBUTED NUMBERS ARE THEN TRANSFORMED
* INTO LOGNORMALLY DISTRIBUTED NUMBERS ( LNORM(J) ) HERE
1   DO 61 J=1,K
    TARA=(Y1(J)/AVEVAR)-DELTAZ/2.
    CALL MDNOR(TARA,TARA1)
    STAR=TARA1*DELTAZ/DELTAY
    CALL MDNRIS(STAR,STAR1,IER)
    LNORM(J)=EXP(2.*VAR1*(STAR1-VAR1))+DELTAY/2.
61  CONTINUE
* THIS SECTION MULTIPLIES THE APPROPRIATE NUMBER OF
* INFORMATION BITS ( R1 (J) ) BY THE PROPER NUMBER OF
* TURBULENCE BITS ( LNORM(J) ), AND THEN ADDS THE
* NOISE TO THE SIGNAL CURRENT. THE RESULTING CURRENT
* LEVEL IS THEN COMPARED TO THE THRESHOLD LEVEL. IF
* IT IS > THAN THRESHOLD A COUNTER IS INITIATED AND
* SUMED. THE TOTAL SUM OF THE COUNTER VARIABLE IS THAN
* DETERMINED. THIS NUMBER EQUALS THE AMOUNT OF 1'S
* THAT THE RECEIVER 'DECIDED' WERE SENT.
    NUM=0
    L=IFIX(GOLD1)
    SUM=0.
    DO 1002 J=1,K
    DO 1003 I=1,L
    IF(R1(I+NUM).GE..5)R1(I+NUM)=1.
    IF(R1(I+NUM).LT..5)R1(I+NUM)=0.
    R2(I+NUM)=LNORM(J)*R1(I+NUM)
    NOIS(I+NUM)=NOIS(I+NUM)*SQRT(THERMN)
    BACK(I+NUM)=BACK(I+NUM)*SQRT(SHOTNO)
    SIGCUR(I+NUM)=SQRT(POWSIG*R2(I+NUM)/RLOAD)
    TOTAL(I+NUM)=SIGCUR(I+NUM)+BACK(I+NUM)+NOIS(I+NUM)
    IF(TOTAL(I+NUM).GE.THRES)RX=1.
    IF(TOTAL(I+NUM).LT.THRES)RX=0.
    IF(R1(I+NUM).EQ.RX)GO TO 1003
    SUM=SUM+1.
1003 CONTINUE
    NUM=NUM+L
1002 CONTINUE
    RETURN
    END
* SUBROUTINE 'DELTA' DETERMINES THE VALUE OF DELTAY IN
* THE GUJAR/KAVANAUGH RELATION
    SUBROUTINE DELTA(VAR,DELTAY)
    DELTAZ=.0001
    GAUSS=3.68-DELTAZ/2.
    VAR1=SQRT(VAR)
    CALL MDNOR(GAUSS,GAUSS1)
    GAUSS2=GAUSS1*DELTAZ
    DELTAY=0.
    B=EXP(2.*VAR1*(3.68-VAR1))

```

```

DO 652 J=1,70000
Y20=B-DELTAY/2.
USA=(1./(2.*VAR1))*ALOG(Y20)+VAR1
CALL MDNR(USA,GUN)
GAUSS4=GAUSS2/GUN
DIF=GAUSS4-DELTAY
IF(DIF.LE.0)GO TO 653
DELTAY=DELTAY+.00000015
652 CONTINUE
653 CONTINUE
RETURN
END

```

Bibliography

1. Mims, Forrest M. III. A Practical Introduction to Lightwave Communications. Indianapolis: H. W. Sams, 1976.
2. Gagliardi, Robert M. and Karp, Sherman. Optical Communications. New York: John Wiley and Sons, 1976.
3. Clifford, S. F. "The Classical Theory of Wave Propagation in a Turbulent Medium," John W. Strohbehn (editor), Laser Beam Propagation in the Atmosphere. Berlin: Springer-Verlag, 1978.
4. Lawrence, Robert S. and Strohbehn, John W. "A Survey of Clear-Air Propagation Effects Relevant to Optical Communications," Proceedings of the IEEE. 58:10, (October 1970).
5. Tatarski, V. I. Wave Propagation in a Turbulent Medium. New York: McGraw-Hill, 1961.
6. Brookner, Eli. "Improved Model for the Structure Constant Variations with Altitude," Proceedings of the IEEE. 10:8, (August 1971).
7. Hoverstein, E. V. and Harger, R. D. "Communications Theory for the Turbulent Atmosphere," Proceedings of the IEEE. 58:10, (October 1970).
8. Cook, Major Richard J., Professor, Physics Department. Personal interview. Air Force Institute of Technology, Wright-Patterson AFB, Ohio, March 1984.
9. Gujar, U. G. and Kavanaugh, R. J. "Generation of Random Signals with Specified Probability Density Functions and Power Density Spectra," IEEE Transactions on Automatic Control. 13:6, (December 1968).
10. Chen, Carson. Active Filter Design. Rochelle Park: Hayden Book Company. 1982.
11. Pratt, William K. Laser Communication Systems. New York: John Wiley and Sons, 1969.
12. Air Force Geophysics Laboratory. Atmospheric Transmittance/Radiance: Computer Code LOWTRAN5. Report Number: AFGL-TR-80-0067; AD A088215. Washington, 1980.

Vita

Jay Nicholas Kanavos was born on 3 November 1958 in Brighton, Massachusetts. He graduated from Tabor Academy, Marion, Massachusetts in 1976. He then attended Norwich University in Northfield, Vermont, from which he received his Bachelor of Science in Electrical Engineering in May 1980. Upon graduation, he received a commission as a Second Lieutenant in the U.S. Air Force. He subsequently completed the Communications-Electronics Officer Course at Keesler AFB, Mississippi in January 1981. He was then assigned to Electronic Systems Division, Hanscom AFB, Massachusetts, where he worked as a Project Officer in the Deputy for Development Plans. In May 1983 he entered the School of Engineering at the Air Force Institute of Technology, Wright-Patterson AFB, Ohio. Captain Kanavos has been selected for assignment to the Command, Control, and Communications branch at Foreign Technology Division Headquarters, Wright-Patterson AFB, Ohio. He is married to Michelle Marie.

Permanent Address: 8 Longmeadow Drive
Wareham, Massachusetts 02571

UNCLASSIFIED

SECURITY CLASSIFICATION OF THIS PAGE

REPORT DOCUMENTATION PAGE

1a. REPORT SECURITY CLASSIFICATION UNCLASSIFIED			1b. RESTRICTIVE MARKINGS		
2a. SECURITY CLASSIFICATION AUTHORITY			3. DISTRIBUTION/AVAILABILITY OF REPORT Approved for public release; distribution unlimited		
2b. DECLASSIFICATION/DOWNGRADING SCHEDULE					
4. PERFORMING ORGANIZATION REPORT NUMBER(S) AFIT/GE/ENG/84D-38			5. MONITORING ORGANIZATION REPORT NUMBER(S)		
6a. NAME OF PERFORMING ORGANIZATION School of Engineering		6b. OFFICE SYMBOL (If applicable) AFIT/ENG	7a. NAME OF MONITORING ORGANIZATION		
6c. ADDRESS (City, State and ZIP Code) Air Force Institute of Technology Wright-Patterson AFB, OH 45433			7b. ADDRESS (City, State and ZIP Code)		
8a. NAME OF FUNDING/SPONSORING ORGANIZATION Air Force Wright Aeronautical Lab.		8b. OFFICE SYMBOL (If applicable) AAAI-1	9. PROCUREMENT INSTRUMENT IDENTIFICATION NUMBER		
8c. ADDRESS (City, State and ZIP Code) AFWAL/AAAI-1 Wright-Patterson AFB, OH 45433			10. SOURCE OF FUNDING NOS.		
11. TITLE (Include Security Classification) See Box 19			PROGRAM ELEMENT NO.	PROJECT NO.	TASK NO.
12. PERSONAL AUTHOR(S) Jay N. Kanavos, B.S.E.E., CAPT, USAF			WORK UNIT NO.		
13a. TYPE OF REPORT MS Thesis		13b. TIME COVERED FROM _____ TO _____	14. DATE OF REPORT (Yr., Mo., Day) 1984 December		15. PAGE COUNT 95
16. SUPPLEMENTARY NOTATION					
17. COSATI CODES			18. SUBJECT TERMS (Continue on reverse if necessary and identify by block number)		
FIELD 17	GROUP 02	SUB. GR.	Optical Communications, Laser Communications, Turbulence.		
19. ABSTRACT (Continue on reverse if necessary and identify by block number)					
Title: THE EFFECTS OF ATMOSPHERIC TURBULENCE ON AN AIR-TO-AIR OPTICAL COMMUNICATION LINK Thesis Chairman: Dr. Vaqar Syed					
20. DISTRIBUTION/AVAILABILITY OF ABSTRACT UNCLASSIFIED/UNLIMITED <input checked="" type="checkbox"/> SAME AS RPT. <input type="checkbox"/> DTIC USERS <input type="checkbox"/>					
21. ABSTRACT SECURITY CLASSIFICATION UNCLASSIFIED			22a. NAME OF RESPONSIBLE INDIVIDUAL Kenneth G. Castor, Major, USAF		
22b. TELEPHONE NUMBER (Include Area Code) 513-255-5533			22c. OFFICE SYMBOL AFIT/ENG		

Approved for public release: IAW AFR 190-17.
LYNN E. WOLANER
Dean for Research and Professional Development
Air Force Institute of Technology (AFIT)
Wright-Patterson AFB OH 45433

UNCLASSIFIED

SECURITY CLASSIFICATION OF THIS PAGE

This report presents an analysis of the performance of an air-to-air optical communication link in the presence of atmospheric turbulence. As aircraft travel through the atmosphere, they encounter regions of atmospheric turbulence. While harmless to radio frequency (RF) communications, these regions of turbulence can cause both intensity and phase fluctuations within an optical beam. As a result, the communication link bit error rate rises.

To evaluate the performance of such a link, a computer simulation was developed. By varying such parameters as the speed of the aircraft, its altitude, and propagation path length, a determination could be made about link performance.

The results obtained from the simulation showed that atmospheric turbulence plays a significant role in determining link performance. It was found that the maximum reliable communication ranges, of those links affected by turbulence (real life situations) were degraded approximately 50 - 60 percent over those links not affected. It was also determined that reasonable changes in aircraft speeds had no significant impact on the bit error rates, while an increase in altitude greatly increased the maximum reliable communication ranges.

UNCLASSIFIED

SECURITY CLASSIFICATION OF THIS PAGE

END

FILMED

4-85

DTIC